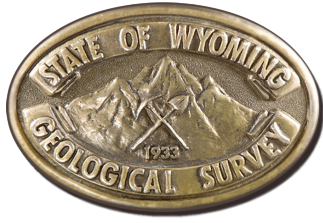


Interpreting the past, providing for the future

Upper Cretaceous Strata in the Powder River Basin: Formation Tops Database, Structure and Thickness Contour Maps, and Associated Well Data

Derek T. Lichtner, Rachel N. Toner, Jackie M. Wrage, and Ranie M. Lynds

Open File Report 2020-9
August 2020



Wyoming State Geological Survey

Erin A. Campbell, Director and State Geologist



Upper Cretaceous Strata in the Powder River Basin: Formation Tops Database, Structure and Thickness Contour Maps, and Associated Well Data

Derek T. Lichtner, Rachel N. Toner, Jackie M. Wrage, and Ranie M. Lynds

Layout by Christina D. George

Open File Report 2020-9
Wyoming State Geological Survey
Laramie, Wyoming: 2020

This Wyoming State Geological Survey (WSGS) Open File Report is preliminary and may require additional compilation and analysis. Additional data and review may be provided in subsequent years. For more information about the WSGS, or to download a copy of this Open File Report, visit www.wsgs.wyo.gov. The WSGS welcomes any comments and suggestions on this research. Please contact the WSGS at 307-766-2286, or email wsgs-info@wyo.gov.

Citation: Lichtner, D.T., Toner, R.N., Wrage, J.M., and Lynds, R.M., 2020, Upper Cretaceous strata in the Powder River Basin —Formation tops database, structure and thickness contour maps, and associated well data: Wyoming State Geological Survey Open File Report 2020-9, 50 p.

Table of Contents

Abstract	1
Introduction	1
Scope of Report	1
Geologic Setting	1
Stratigraphy	3
Methods	7
Type Log Signatures	7
Data Acquisition and Quality Control	10
Database	11
Contouring Methods	11
Sources of Uncertainty	11
Results	12
General Structure and Thickness Trends	12
Trends by Formation	14
Summary	45
Acknowledgments	45
References	46

List of Tables

Table 1. Top 10 oil- and gas-producing reservoirs in the PRB in 2019.	1
---	---

List of Figures

Figure 1. Powder River Basin bedrock geology and study area map	2
Figure 2. Generalized cross section of the Powder River Basin.	3
Figure 3. Correlation of Upper Cretaceous strata in the Powder River Basin	4
Figure 4. Type log for the southwestern Powder River Basin, API 49-025-23801.	8
Figure 5. Type log for the northwestern Powder River Basin, API 49-033-28167.	8
Figure 6. Type log for the northeastern Powder River Basin, API 49-005-54781.	8
Figure 7. Type log for the southeastern Powder River Basin, API 49-027-26624.	9
Figure 8. Type log for the central Powder River Basin, API 49-005-61828.	9
Figure 9. Generalized confidence in contour map predictions	13
Figure 10. Structure map of top of the Muddy Sandstone	17
Figure 11. Structure map of top of the Mowry Shale	18

Figure 12. Thickness of the combined Mowry-Shell Creek interval	19
Figure 13. Structure map of top of the Belle Fourche	20
Figure 14. Thickness of the Belle Fourche	21
Figure 15. Structure map of top of the Greenhorn.	22
Figure 16. Thickness of the Greenhorn	23
Figure 17. Structure map of top of the Pool Creek.	24
Figure 18. Thickness of the Pool Creek	25
Figure 19. Structure map of top of the combined Turner-Wall Creek	26
Figure 20. Thickness of the combined Turner-Wall Creek.	27
Figure 21. Structure map of top of the combined Sage Break-Carlile.	28
Figure 22. Thickness of the Sage Breaks.	29
Figure 23. Structure map of top of the Niobrara.	30
Figure 24. Thickness of the Niobrara.	31
Figure 25. Structure map of top of the Shannon Sandstone.	32
Figure 26. Thickness of the Shannon Sandstone	33
Figure 27. Structure map of top of the Sussex Sandstone.	34
Figure 28. Thickness of the Sussex Sandstone	35
Figure 29. Structure map of top of the combined Red Bird-Parkman Sandstone.	36
Figure 30. Thickness of the combined Red Bird-Parkman Sandstone.	37
Figure 31. Structure map of top of the Teapot Sandstone.	38
Figure 32. Thickness of the Teapot Sandstone	39
Figure 33. Structure map of top of the Teckla Sandstone.	40
Figure 34. Thickness of the Teckla Sandstone	41
Figure 35. Structure map of base of the Fox Hills Sandstone	42
Figure 36. Structure map of top of the Fox Hills Sandstone.	43
Figure 37. Thickness of the Fox Hills Sandstone.	44

ABSTRACT

Upper Cretaceous strata in the Powder River Basin of northeastern Wyoming and southeastern Montana contain some of Wyoming's most prolific oil and gas reservoirs as well as significant petroleum-generating source rocks. Using geophysical well logs from more than 2,200 oil and gas wells, key horizons within the Upper Cretaceous strata were identified throughout the basin, with the primary goal of a publicly available dataset containing depth-to-formation and assorted well data, including location, depth, datum, well type, and well class, for the Lower Cretaceous Muddy Sandstone through the Upper Cretaceous Fox Hills Sandstone. Compiled data were inspected for accuracy by comparison with primary documents. Contour maps derived from the formation depths illustrate basin-wide trends in formation depth and thickness. Subsurface interpretations and spatial contour data are available on the Wyoming State Geological Survey [publications webpage](#) and [Interactive Oil and Gas Map of Wyoming](#).

INTRODUCTION

Scope of Report

The Powder River Basin (PRB) ranks first in oil and second in natural gas production among basins in Wyoming (Wyoming Oil and Gas Conservation Commission, 2020). Since 2014, the PRB has accounted for more than half of Wyoming's total oil production. Increased production in the PRB over the last decade was due largely to the development of hydraulic fracturing and horizontal drilling, which led to an industry-wide shift in exploration targets from conventional, high-porosity reservoirs within spatially defined traps to geographically extensive, low-porosity and permeability unconventional reservoirs. In the PRB, these predominantly Upper Cretaceous unconventional reservoirs (table 1) include continuous accumulations in the Mowry Shale; the Wall Creek Member of the Frontier Formation; the Turner Sandy Member of the Carlile Shale; the Niobrara Formation; the Shannon Sandstone, Sussex Sandstone, and Niobrara members of the Cody Shale; and the Parkman Sandstone and Teapot Sandstone members of the Mesaverde Formation (Bottjer and others, 2017; Zborowski, 2018; Kegel and others, 2019; Toner and others, 2019).

To better understand the stratigraphy and geometry of these unconventional tight oil and gas reservoirs, their source rocks, and intervening strata, the depths to Upper Cretaceous stratigraphic surfaces were interpreted in more than 2,200 geophysical well logs. These depth interpretations, or "formation tops," also include the bases of those strata with lower contacts not defined by the top of another formation. The formation tops were used to develop type logs, create contour maps of formation depth and thickness, and populate a publicly available database.

Geologic Setting

The geographic extent of the Wyoming portion of the PRB is defined by Laramide-age uplifts: the Bighorn Mountains, Casper Arch, Laramie Mountains, Hartville Uplift, and Black Hills (fig. 1). The Miles City Arch defines the northern extent of the PRB in Montana. The PRB is asymmetric, with steeply dipping strata along the western margin and shallow dips in the eastern basin (fig. 2). The basin axis trends northwest-southeast, and is located immediately east of and subparallel to the Bighorn Mountains. The structural relief of Precambrian rocks, from the basin axis to the basin's western margin, exceeds 6,000 m (20,000 ft; Blackstone, 1993).

Table 1. Top 10 oil- and gas-producing reservoirs in the PRB in 2019, excluding coalbed methane reservoirs (Wyoming Oil and Gas Conservation Commission, 2020).

Top oil-producing reservoirs	Top gas-producing reservoirs
Turner	Turner
Parkman	Niobrara
Niobrara	Frontier, unspecified
Frontier, unspecified	Parkman
Wall Creek, combined	Mowry
Minnelusa	Sussex
Shannon	Muddy
Teapot	Teapot
Sussex	Shannon
Muddy	Dakota

The PRB contains nearly 5,500 m (18,000 ft) of Cambrian- to Eocene-age sedimentary deposits. Paleozoic strata were deposited along the passive western margin of the North American craton (Boyd, 1993). Triassic and Jurassic strata were subsequently deposited in marginal marine and non-marine environments (Picard, 1993).

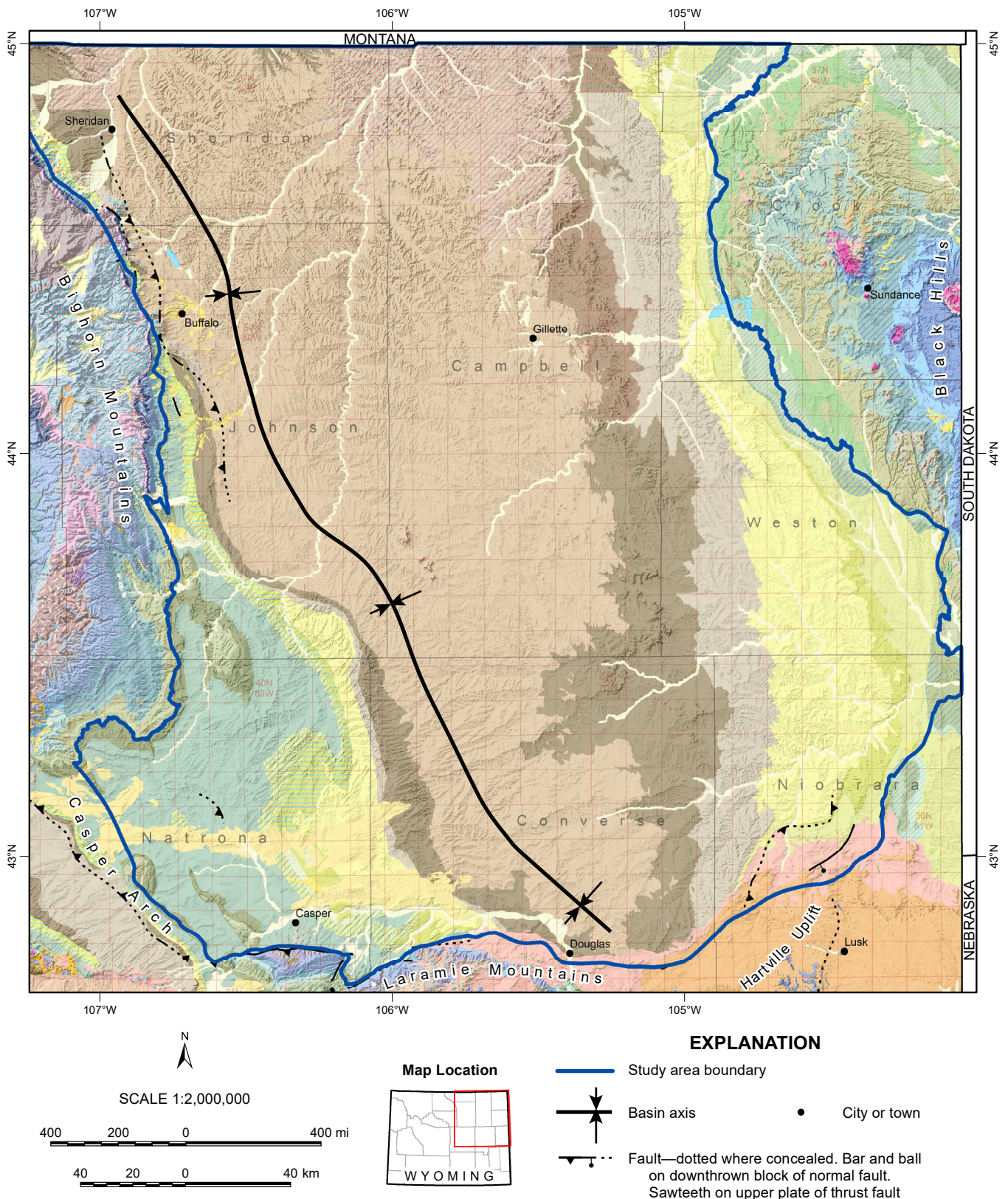


Figure 1. Powder River Basin bedrock geology and study area map. Geologic unit ages and colors follow Love and Christiansen (1985): Paleogene—browns, oranges, and pinks; Mesozoic—yellows and greens; Paleozoic—blues and purples. Precambrian-cored Laramide uplifts bound the basin.

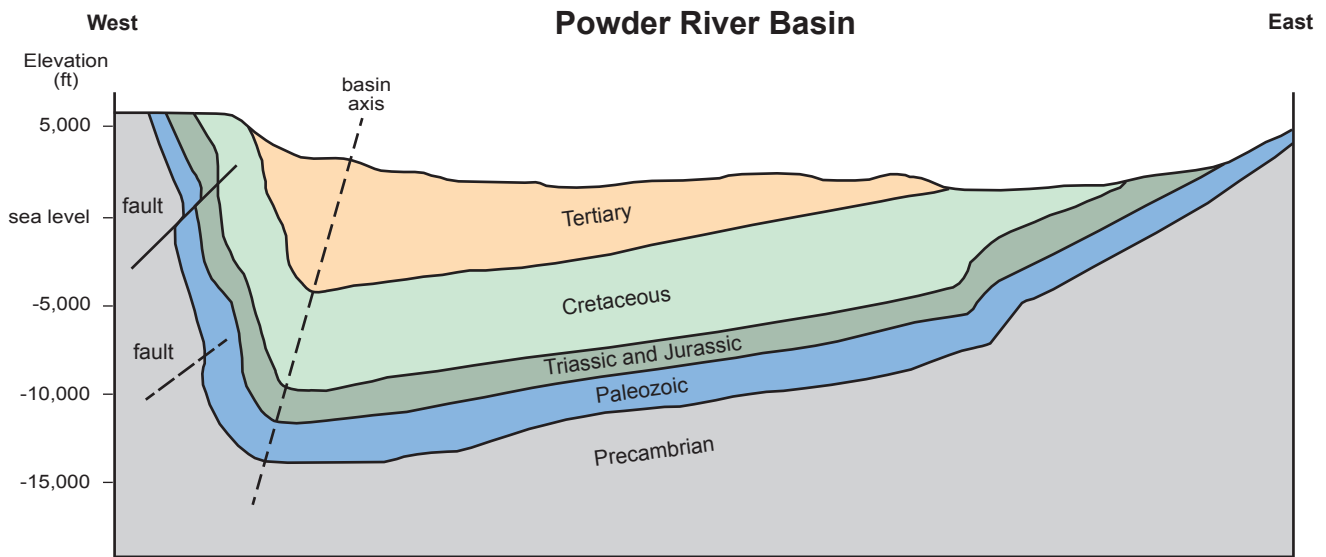


Figure 2. Generalized cross section of the Powder River Basin, modified from Anna (2010).

The Cretaceous strata of the PRB record in detail alternating periods of marine and marginal-marine deposition. Prior to Laramide deformation, the PRB was part of the extensive foreland basin east of the Sevier orogenic belt (Royse, 1993; Steidtmann, 1993). Throughout much of the Late Cretaceous, this basin was flooded by the epicontinental Western Interior Seaway. Fluctuating relative sea level and sediment supply, combined with the accommodation space provided by Sevier deformation, produced a thick, complex sequence of intercalated shallow marine, deltaic, and coastal sediments throughout western and central North America.

Near the end of the Cretaceous, the Laramide orogeny partitioned the Sevier foreland in Wyoming into discrete basins separated by basement-cored uplifts. Uppermost Cretaceous and Paleogene strata in the PRB and other Laramide basins were deposited in an intracontinental setting (Brown, 1993; Lillegraven, 1993).

Stratigraphy

The PRB Upper Cretaceous section conformably overlies Lower Cretaceous units and is conformably overlain by Paleogene units. Several regional disconformities exist in the basin's Cenomanian and Turonian sediments (Weimer and Flexer, 1985; Merewether, 1996; Merewether and others, 2007). Upper Cretaceous strata in the PRB consist of siliciclastic and carbonate rocks, with minor intervening bentonite and coal (fig. 3). The geologic units examined in this study are discussed below. The Lower Cretaceous Muddy Sandstone is included in order to identify the base of the Upper Cretaceous section.

Muddy Sandstone (Muddy). The Muddy Sandstone consists of sandstone and mudstone deposited in fluvial, estuarine, and nearshore environments during seaway regression (Anna, 2010). The Muddy is historically a prolific oil producer, with producing intervals typically associated with incised valley fill systems (Dolson and others, 1991). The Muddy is conformably overlain by the Shell Creek Shale, a soft black shale (Eicher, 1962). The top of the Shell Creek was not identified in the subsurface in this study. The Shell Creek Shale is conformably overlain by the Mowry Shale.

Mowry Shale (Mowry). The Mowry Shale consists of organic-rich, siliceous shale and interbedded bentonite deposited during maximum marine transgression (Merewether, 1996). The Mowry is regarded as an important source rock for both Lower and Upper Cretaceous PRB reservoirs, with one of the highest average total organic carbon content of Cretaceous shales in the region (Momper and Williams, 1984; Dolton and others, 1990; Rahman and others, 2016; Hart and others, 2019). The Mowry Shale is also being developed as an unconventional reservoir (Anna, 2010; Purvis and others, 2017; Cuddus and others, 2019). The Mowry is conformably overlain by the Belle Fourche Formation, or Belle Fourche Member of the Frontier Formation.

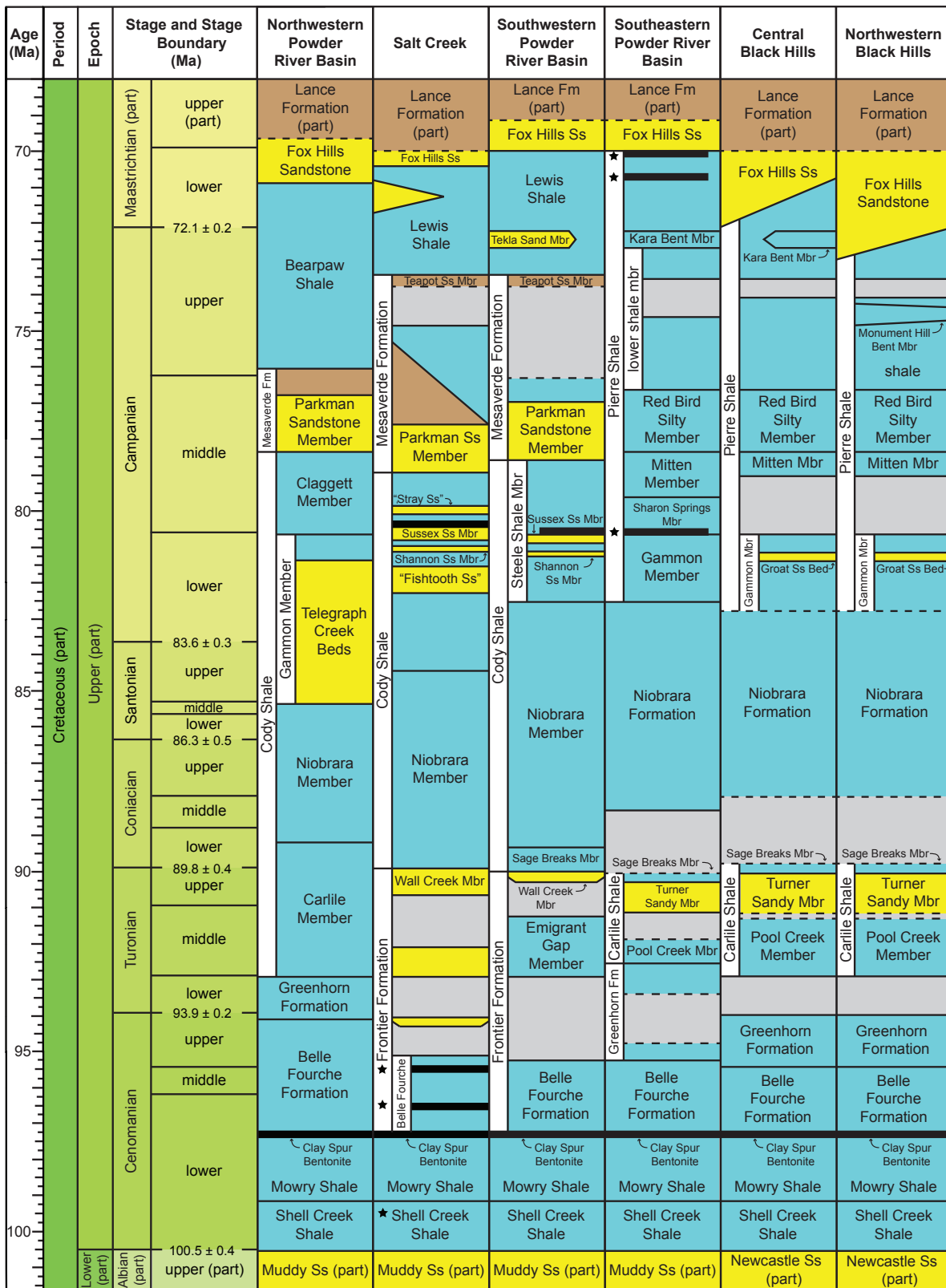


Figure 3. Correlation of Upper Cretaceous strata in the PRB, modified from Lynds and Slattery (2017). Age boundaries are solid where certain, dashed where uncertain or interpreted. Colors correspond to generalized depositional environments: brown is terrestrial and transitional marine, yellow is nearshore to transitional marine, and blue is offshore. Gray indicates missing or condensed section. Thick black lines are bentonite beds. A black star marks the approximate location of a radiometric age sample. Abbreviations used are bentonite (Bent), formation (Fm), member (Mbr), and sandstone (Ss).

Belle Fourche Shale or Belle Fourche Member of the Frontier Formation (Belle Fourche). The Belle Fourche Shale is recognized in the eastern PRB and is considered a member of the Frontier Formation in the western PRB. The Belle Fourche Shale is a noncalcareous shale interbedded with bentonite that was deposited in an offshore marine environment (Cobban, 1952; Robinson and others, 1964). The Belle Fourche Member of the Frontier Formation is the nearshore and marginal marine equivalent, consisting of a variety of siliciclastic lithologies, from mudstone to partly conglomeratic sandstone (Merewether and others, 1979). The Belle Fourche is conformably overlain by the Greenhorn Formation in the northeast, disconformably overlain by the Greenhorn Formation in the east and southeast, and disconformably overlain by either the Emigrant Gap or Wall Creek members of the Frontier Formation in the west.

Greenhorn Formation (Greenhorn). The Greenhorn Formation is restricted to the eastern and northwestern PRB, and is composed primarily of calcareous shale and limestone deposited in an open-marine environment (Macdonald and Byers, 1988). Where present in the basin, the Greenhorn is conformably overlain by the Carlile Shale. In the southwestern portion of the PRB, the Greenhorn is absent due to the late Cenomanian and early Turonian regional hiatus that separates the Belle Fourche Member of the Frontier Formation from the the overlying Emigrant Gap Member.

Pool Creek Member of the Carlile Shale (Pool Creek). The Pool Creek consists of soft, concretion-bearing shale interbedded with occasional limestone and bentonite, and was deposited in shelf and slope environments (Cobban, 1951; Robinson and others, 1964). The Pool Creek Member is present in the eastern PRB and grades southwest into the Emigrant Gap Member of the Frontier Formation, which consists of a basal conglomeratic sandstone and overlying mudstone, siltstone, and sandstone deposited mainly in nearshore environments (Merewether and others, 1979). The Pool Creek was partly to completely removed by erosion in Campbell, Weston, Converse, and Niobrara counties (Merewether and others, 1977a; Weimer and Flexer, 1985; Fox, 1993a, b, c, d). The Pool Creek is disconformably overlain by the Turner Sandy Member of the Carlile Shale, and in the west the Emigrant Gap Member is disconformably overlain by the Wall Creek Member of the Frontier Formation. The top of the Emigrant Gap Member was not identified in this study.

Turner Sandy Member of the Carlile Shale (Turner) and Wall Creek Member of the Frontier Formation (Wall Creek). The Turner Sandy Member of the Carlile Shale is composed of a thin, locally medium-grained sandstone overlain by interbedded noncalcareous shale, argillaceous siltstone, and minor sandstone, deposited mainly in estuary, nearshore, and shelf environments (Merewether and others, 1979; Weimer and Flexer, 1985; Heger, 2016). The Turner is present in the eastern PRB and is time-equivalent to the Wall Creek Member of the Frontier Formation to the west. The Wall Creek consists of several coarsening-upward packages of siltstone to coarse-grained sandstone deposited in nearshore and delta-front environments (Merewether and others, 1979; Dellenbach, 2019). Both the Wall Creek and Turner in the PRB are significant unconventional plays (Toner, 2019). The base of both units is a regional disconformity, indicating subaerial exposure and extensive erosion during middle and late Turonian time (Weimner and Flexer, 1985). The Turner is conformably overlain by the Sage Breaks Member of the Carlile Shale, and the Wall Creek is conformably overlain by the Sage Breaks Member of the Cody Shale.

Sage Breaks Member of the Carlile or Cody shales (Sage Breaks), and Carlile Member of the Cody Shale (Carlile). The Sage Breaks Member of the Carlile or Cody shales consists of noncalcareous to slightly calcareous concretion-bearing shale deposited in shelf and slope environments (Cobban, 1951; Robinson and others, 1964). Where the Sage Breaks Member is not present, the top of the undivided Carlile Shale or Carlile Member of the Cody Shale is considered its stratigraphic equivalent. Concretion-bearing shale, similar to that of the Sage Breaks, crops out in the upper part of the Carlile in the northwestern PRB (Merewether, 1996). The Sage Breaks and Carlile are disconformably overlain by the Niobrara Formation or Niobrara Member of the Cody Shale.

Niobrara Formation or Niobrara Member of the Cody Shale (Niobrara). The Niobrara is composed of a series of clayey limestone, shale, bioturbated chalk, and thin beds of bentonite deposited in an open-marine environment during a major marine transgression and subsequent regression (Robinson and others, 1964; Weimer and Flexer, 1985). The Niobrara is considered an important hydrocarbon source rock for Upper Cretaceous reservoirs in the PRB (Landon and others, 2001; Anna, 2010; Rahman and others, 2016; Hart and others, 2019; Kondakci, 2019). The Niobrara is also a burgeoning unconventional reservoir (Taylor and Sonnenberg, 2014; Sonnenberg, 2018). The Niobrara is divided into three chalky marl benches, of which the “B” and “C” benches are typically the reservoir targets (Taylor, 2012; Kondakci, 2019; Stewart, 2019). The disconformity at the base of the Niobrara represents a regional hiatus in Coniacian time;

erosion of the underlying Sage Breaks Member was greatest in an elongate region trending northwest from southern Niobrara County to southwestern Campbell County (Weimer and Flexer, 1985). The Niobrara is conformably overlain by and interfingers with the Gammon Member of the Pierre Shale in the east and by lower shale members of the Cody Shale in the west.

Shannon Sandstone Member of the Cody Shale (Shannon). The Shannon consists of sandstone and occasional interbedded siltstone and shale deposited in shoreface and shelf-bar environments indicative of an overall eastward progradation of clastic sediments (Tillman and Martinsen, 1984; Kaykun, 2018). The Shannon is separated from the overlying Sussex Sandstone Member by approximately 100 m (330 ft) of the Steele Shale Member of the Cody Shale. Observation of the Shannon in the subsurface was limited to the western PRB.

Sussex Sandstone Member of the Cody Shale (Sussex). The Sussex is composed of sandstone and lesser shale and siltstone, and is typically interpreted as having been deposited as bar complexes in a shelf environment (Berg, 1975). Oil production is often associated with bioturbated sandstone facies (Bottjer and others, 2014). The top of the Sussex in the subsurface is delineated by the Ardmore bentonite bed, which is in turn overlain by the upper Pierre Shale in the east or the upper Steele Shale Member of the Cody Shale in the west. Observation of the Sussex in the subsurface was limited to the southwestern and central PRB.

Red Bird Silty Member of the Pierre Shale (Red Bird) and Parkman Sandstone Member of the Mesaverde Formation (Parkman). The Parkman is composed of interbedded fine-grained sandstone and carbonaceous shale with local coal beds, and was deposited in the marine and marginal-marine environments of a prograding delta (Gill and Cobban, 1973). Oil is typically produced from stratigraphic traps associated with marine bar sandstones or incised valley development (Anna, 2010; Steidtmann, 2019). The Red Bird is found in the eastern PRB and consists of concretion-bearing silty and sandy shale deposited in a shelf environment (Robinson and others, 1964; Gill and others, 1966). It is laterally continuous with and chronologically equivalent to the Parkman, which is found in the western PRB. The Red Bird is conformably overlain by a lower unnamed part of the Pierre Shale, and conformably overlies the Mitten Member of the Pierre Shale (Mitten). The gray Mitten shale is time-equivalent to the upper Cody Shale, but was not investigated in this study except to delineate the base of the Red Bird. The Parkman is conformably overlain by an unnamed shale of the Mesaverde Formation, which is disconformably overlain by the Teapot Sandstone Member. The base of the Parkman is conformable with the uppermost shale members of the Cody Shale.

Teapot Sandstone Member of the Mesaverde Formation (Teapot). The Teapot is a carbonaceous sandstone with local silty to sandy shale and coal (Curry, 1976). The Teapot is interpreted as a progradational sequence of marine to nonmarine lithofacies that grades eastward into an unnamed member of the Pierre Shale (Gill and Cobban, 1973). The base of the Teapot is disconformable with an unnamed shale of the Mesaverde Formation. The Teapot is conformably overlain by the Lewis Shale in most of the basin, which is composed of mudstone to siltstone interbedded with sandstone and rare limestone, and contains the Teckla Sandstone Member. In the northwestern PRB, the Mesaverde Formation is overlain by the Bearpaw Shale.

Teckla Sandstone Member of the Lewis Shale (Teckla). The Teckla was deposited in nearshore and deltaic environments and consists of either two sandstone units separated by bentonitic shale, or away from its depocenter, one sandstone unit (Runge and others, 1973). Due to differences in sedimentation and accommodation space, the southern portion of the delta system is considered to contain sandstones of higher reservoir quality (Anna, 2010). Present in the southwestern PRB, the Teckla is conformably bound by the unnamed upper and lower parts of the Lewis Shale, also a potential source rock and reservoir.

Fox Hills Sandstone (Fox Hills). The Fox Hills consists of one or more coarsening-upward units of fine- to medium-grained sandstone interbedded with sandy shale (Robinson and others, 1964; Gill and Cobban, 1966). It was deposited in nearshore and deltaic environments, and records the final retreat of the Western Interior Seaway (Merewether, 1996). The base of the Fox Hills is conformable with the Bearpaw and Lewis shales in the western PRB and with the uppermost Pierre Shale (Pierre) in the east. It is conformably overlain and grades into the nonmarine strata of the Lance Formation (Robinson and others, 1964). The Fox Hills is the uppermost unit investigated in this study.

METHODS

Oil and gas wells in the PRB were chosen for study based on their location in the basin and the quality of available associated data. Formation tops were interpreted in IHS Petra 4.3.0 using depth-registered raster logs. Five geophysical type logs guided subsequent subsurface interpretations for at least one well in every PRB township where data are available. The resulting dataset correlates subsurface formation tops between more than 2,200 wells throughout the basin. Additional well data associated with the completion and logging of each well were compiled and inspected for accuracy before use in subsurface interpretation. A relational database was assembled from the resultant stratigraphic interpretations and associated well data. Formation tops were interpolated between wells to generate contour maps of formation structure and thickness.

Type Log Signatures

Formation tops were identified for the interval from the Lower Cretaceous Muddy Sandstone through the Upper Cretaceous Fox Hills Sandstone. Previous work, primarily by Merewether and others (1977a,b,c) and Fox (1993a,b,c,d), as well as by Robinson and others (1964), Runge and others (1973), Merewether (1980, 1996), Weimer and Flexer (1985), Van Wagoner and others (1990), and Taylor (2012), guided the identification of formation picks.

Five type logs show the characteristic spontaneous potential (SP), resistivity, and gamma log signatures used to identify the formation picks in this study (figs. 4–8). Significant departures from the type log signature in other wells may exist due to local variations in geology or pore fluids.

Muddy. The Muddy log signature is blocky with elevated resistivity, low gamma, and slight negative SP inflection values. The Muddy is not present in all locations, and the stratigraphically equivalent base of the combined Mowry-Shell Creek interval was chosen in these rare occurrences.

Mowry. The Mowry is readily identified by a distinct comb-shaped, elevated resistivity curve. Occasional gamma spikes, associated with bentonite layers, are present throughout. The geographically extensive Clay Spur bentonite bed marks the top of the Mowry.

Belle Fourche. The Belle Fourche is characterized by several packages of increasing-upward, generally moderate resistivity and decreasing-upward gamma and SP. Common gamma spikes, associated with bentonite layers, are present throughout.

Greenhorn. The Greenhorn is identified by the combination of somewhat elevated gamma compared to the underlying Belle Fourche, as well as generally more uniform gamma, resistivity, and SP curves. In some logs resistivity increases upward and gamma and SP decrease upward. In other logs, gamma and SP increase and then decrease upward, whereas resistivity follows the opposite trend. The top of the Greenhorn is marked by a distinct high-resistivity, low-gamma ledge.

Pool Creek. The Pool Creek is most easily identified by the relatively uniform gamma, SP, and resistivity curves between the Greenhorn Formation and Turner Sandy Member.

Turner and Wall Creek. The elevated resistivity and decreased, moderately serrated gamma curves of the Turner contrast with the relatively muted curves of the underlying Pool Creek and overlying Sage Breaks. The Wall Creek log signature is similar to that of the Turner, but often with a lower gamma and higher resistivity due to higher sand content.

Sage Breaks and Carlile. The Sage Breaks is most easily recognized by the uniform low-resistivity curve between the moderately serrated signature of the Turner and the distinctive log signature of the Niobrara Formation. The equivalent strata of the upper Carlile have similarly uniform log signatures.

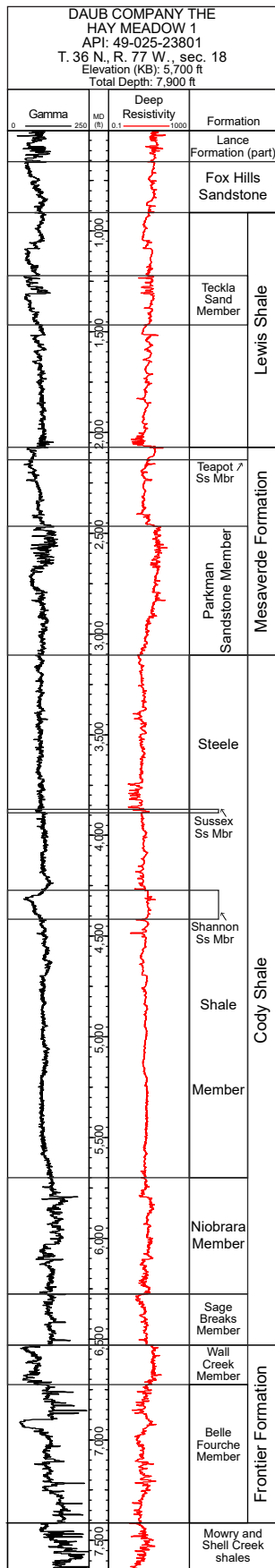


Figure 4. Type log for the southwestern PRB, API 49-025-23801.

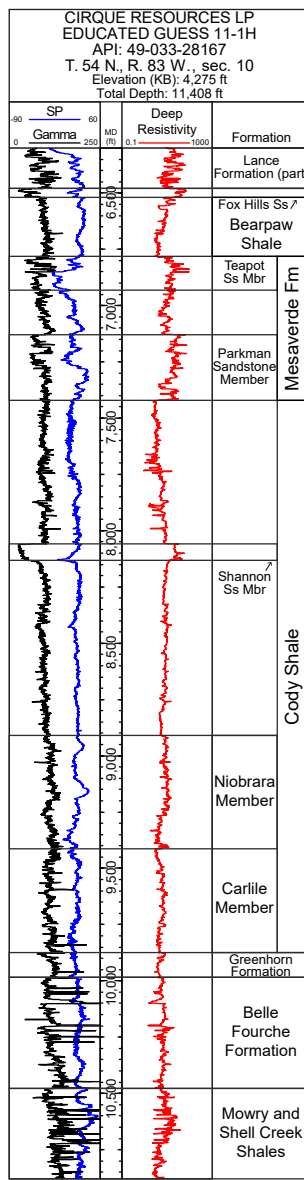


Figure 5. Type log for the northwestern PRB, API 49-033-28167.

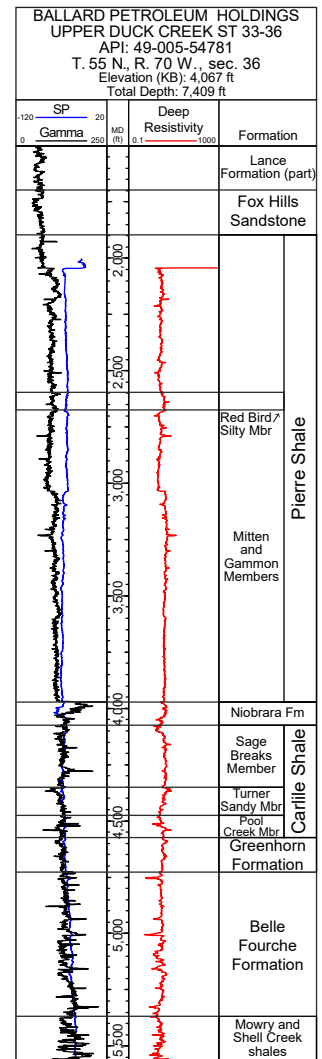


Figure 6. Type log for the northeastern PRB, API 49-005-54781.

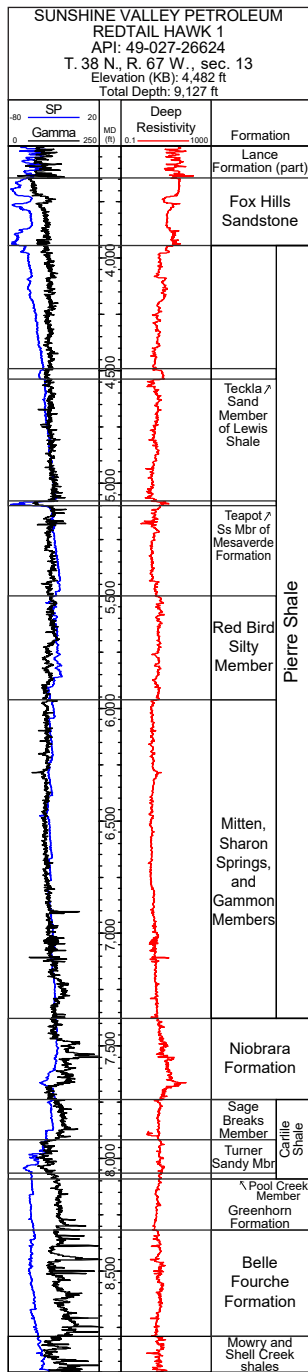


Figure 7. Type log for the southeastern PRB, API 49-027-26624.

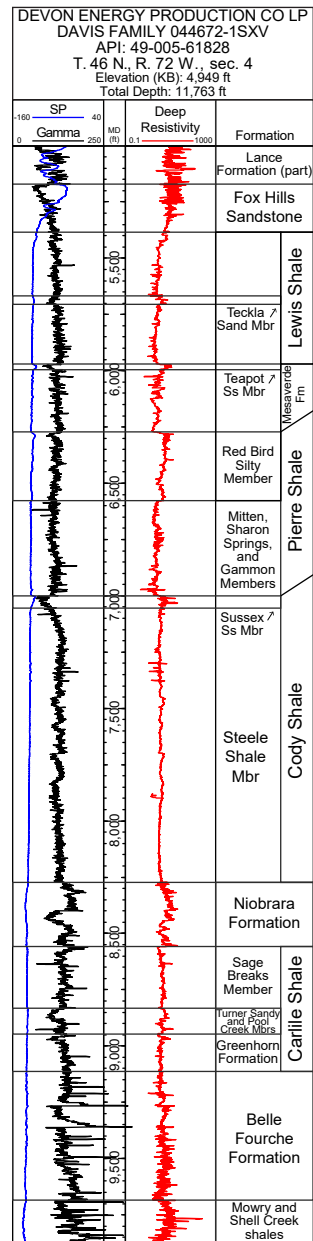


Figure 8. Type log for the central PRB, API 49-005-61828.

Niobrara. The Niobrara log signature is indicated by a distinct increase in resistivity combined with parallel increases in gamma and SP. The base of the Niobrara is marked by a sharp resistivity spike.

Shannon. The Shannon log signature displays elevated resistivity and decreased gamma and SP. In some logs the gamma curve displays the decreasing-upward trend typical of a coarsening-upward sandstone. The Shannon is most recognizable in the Powell oil and gas field of northwestern Converse County; elsewhere it is considered present only in wells with a clear log signature. The Shannon is separated from the overlying Sussex by an unnamed shale containing a cluster of gamma spikes associated with bentonite beds.

Sussex. The top of the Sussex is readily identified by the sharp increase in gamma associated with the Ardmore bentonite bed. The body of the Sussex is less easily recognized, and to varying degrees exhibits increasing-upward and somewhat elevated resistivity, elevated SP, and decreased gamma.

Parkman. The base of the Parkman is defined by the first of several packages of decreasing-upward gamma and increasing-upward resistivity. Superimposed on these packages, which vary in number, is an overall increasing-upward resistivity trend. SP tends to be elevated in the lower parts of the Parkman. At the top of the uppermost sandstone package, the somewhat serrated Parkman log signature abruptly transitions to the more subdued curves of the overlying main body of the Mesaverde Formation. In some locations an additional subdued sandstone signature was observed above the Parkman. This study does not consider this intermittent sand as part of the Parkman.

Red Bird. The top of the Mitten in the eastern PRB corresponds to the base of the Red Bird, and the Mitten was delineated in this study to determine the thickness of the Red Bird. The Mitten has a high-gamma, low-resistivity, uniform log signature typical of PRB shales. The Red Bird log signature is similar to that of the Parkman but overall less responsive. The region of elevated resistivity associated with the Red Bird is generally blockier and more uniform than that of the Parkman.

Teapot. The Teapot is yet another interval of increasing-upward elevated resistivity and decreased gamma typical of PRB sandstones. The base of the Teapot is in some wells difficult to distinguish from the generally coarsening-upward trend of the underlying unnamed shale of the Mesaverde Formation. However, the top of the Teapot is clearly marked by an abrupt transition to the uniform low resistivity, high gamma of the overlying Lewis Shale or Bearpaw Shale. In locations where a relatively subtle resistivity signature was observed, but without a corresponding SP or gamma inflection, the Teapot was considered absent.

Teckla. The Teckla log signature consists of one or two closely spaced sandstone packages of elevated resistivity and decreased gamma separated by a bentonitic shale layer. In some wells the gamma signature decreases upward, as is typical of Upper Cretaceous sandstones in the PRB, but the resistivity signature of the Teckla is generally blockier than that of the Teapot and other PRB sandstones.

Fox Hills. This study defines the lower contact of the Fox Hills as the top of the stratigraphically equivalent Bearpaw (northwestern PRB), Pierre (eastern PRB), and Lewis (western PRB) shales, which display typical shale log signatures, with high gamma and low resistivity and an overall gradually coarsening-upward trend. The base of the Fox Hills is the first of one or more clustered packages of decreasing-upward gamma and increasing-upward resistivity. Because the number of distinct packages and the spacing between them varies throughout the PRB, there is often no clear method for differentiating a minor sandstone in the underlying Pierre or Lewis shales from the lowermost Fox Hills sand. The top of the Fox Hills, in contrast, is easily identified by the transition to the chaotic, strongly serrated gamma and resistivity signatures of the overlying Lance Formation.

Data Acquisition and Quality Control

For all wells with subsurface formation tops, associated well data were compiled from the Wyoming Oil and Gas Conservation Commission (WOGCC) publicly available dataset. Where public data were unavailable, well logs from IHS's proprietary database were referenced, but proprietary data are neither reported nor reproduced. To reduce inaccuracies

inherent in the data reported to the WOGCC, the authors conducted several rounds of quality control to verify well locations, well depths, and elevation datums using well logs, completion reports, historical card files, directional surveys, and digital elevation models.

Database

The formation tops were exported from Petra and imported into an enterprise ArcGIS Spatial Database Engine (SDE) using an SQL Server platform. The respective associated well data were also imported into SDE. Domains were established to limit data input errors. Database views were created for spatially displaying complex queries and joins of multiple data tables. The combination of SDE's spatial and relational functionality allows the subsurface interpretations and associated well data to be organized and displayed in a robust, responsive format.

Contouring Methods

To illustrate basin-wide trends in the PRB's Upper Cretaceous geology, contour maps were created by interpolating formation tops and thickness between dataset wells.

Subsea depth to a formation was calculated by subtracting the interpreted depth to each formation top from the geophysical well log elevation datum. Regional bedrock geologic maps (Love and Christiansen, 1985; Hallberg and others, 2002; Ver Ploeg and Boyd, 2002, 2003; Ver Ploeg and others, 2004; Hunter and others, 2005; McLaughlin and Ver Ploeg, 2006, 2008; Sutherland, 2007, 2008; Wittke, 2007; Johnson and Micale, 2008; McLaughlin and others, 2011) and digital elevation models (U.S. Geological Survey, 2009) were used to constrain the elevation of formation tops where units intersect the ground surface. Surface data points were sampled at an interval equal to the average nearest neighbor of the geographic distribution of well data. Structure contour maps were interpolated in ArcGIS 10.7.1 using simple kriging of the formation-top subsea depths after second-order trend removal (Oliver and Webster, 2014; Olea, 2009). Because semivariogram models of representative subsets of data indicate that the variation in subsea depths throughout the basin is several orders of magnitude greater than the estimated nugget, semivariograms were fit by a stable model with a constant nugget of zero.

Formation thickness was calculated at each well by differencing the appropriate stratigraphic horizons. Because no correction was made for dip, this study's thickness measurements are isochores. Unit thickness was contoured with simple kriging of the dataset after log transformation and first-order trend removal. Semivariograms were fit by a stable model with a constant nugget chosen based on model fits to several data subsets. For both structure and thickness maps, the contour-line overlays were simplified and smoothed.

The extent of each contour map is dictated by basin-margin structure and data availability for each formation. In the north, correlations are restricted to the Wyoming portion of the PRB. Along the eastern and western margins of the PRB, contours are bound by formation outcrop. In the southwest, the contours terminate 5–15 km (3.1–9.3 mi) northeast of the surface expression of the Casper Arch thrust, where dataset density is insufficient to capture mesoscale geologic structure. In the south-central PRB, contours extend as far as the faults bounding Casper Mountain and the Laramie Mountains. Near the southeastern basin margin contours end at the approximate crest of the Old Woman Anticline. Elsewhere, the absence of data for a formation limits contour extent.

Sources of Uncertainty

Uncertainty in subsurface interpretation is introduced during data acquisition, compilation, and manipulation. Uncertainty is also present due to variability in geologic process and scale, as well as geologist interpretation. Below is a list of the primary sources of uncertainty identified during this study and the efforts made to reduce the uncertainty when possible.

Data reporting. Well data can be inaccurately reported to the WOGCC by drillers, loggers, and operators. Data entry errors also exist when converting scanned information to a digital format. This study's quality-control procedures corrected well datums, which in rare cases differed from the true elevation datum by more than 30 m (100 ft). Well locations are sometimes inconsistent with permits, completion reports, aerial photos, and associated geophysical well logs. Even after

thorough review and correction of the dataset, some datum and location inaccuracies may persist due to unknown errors in the original reported data.

Natural well drift. Undocumented natural drift of measured depth from true vertical depth introduces uncertainty in subsea depths. For wells with no available directional surveys, the depth to a formation measured from a well log cannot be corrected to the true vertical depth. As the magnitude of drift increases with depth, so does this uncertainty. Top identification in this study was limited to vertical wells or the vertical portion of directional and horizontal wells.

Subsurface structure. Faults, folds, and regional lineaments with no surface expression can influence geologic interpretation. Without seismic or core data to constrain such structures, correlations may be forced or inaccurate.

Steep dips. Where strata are steeply dipping, the apparent thickness measured from a well log overestimates the true thickness. Because no correction was made for apparent thickness, all thickness measurements should be considered isochore values. Furthermore, if both a well's location is inaccurate and the strata of interest are steeply dipping, error proportional to the dip angle is introduced, causing the depth to formation at the incorrectly plotted location to deviate from the true vertical depth.

Data density. In portions of the basin where subsurface well data are scarce, meso- and microscale variability from faults, folds, and heterogeneity in sedimentological processes is not adequately represented.

Confidence of contour map predictions. Where data are sparse, geostatistical methods can estimate the confidence of contour map predictions (fig. 9). The confidence in this study's predicted subsea depths in the vicinity of a database well is generally high, within several meters (feet to tens of feet). With increasing distance from a database well, the confidence in contours of subsea depth is lower and predicted depth of a formation may be reliable within only a hundred meters or so (several hundred feet). In addition to data density, geologic structure and natural drift, particularly for deeper formation tops, influence the confidence in predicted depths. Confidence is particularly low along the basin axis, where data are sparse and the basin is deep, and in the Casper Arch region, where data density is too low to adequately capture the complexity of the geologic structure.

Geologic interpretation. Subsurface interpretation varies by geologist and can be influenced by referenced publications, the scale of investigation, well logs available to each geologist, and unknown structural features. In addition, the interpretation of PRB subsurface geology is complicated by changing nomenclature, interfingering lithologies, and dissimilar geophysical methods.

RESULTS

General Structure and Thickness Trends

Structure. Contour maps of depth to Upper Cretaceous strata in the PRB reflect the basin's asymmetric geometry. Strata are shallowest near the basin margins, where many of the formations are exposed at the surface. Formations are deepest east of the Bighorn Mountains along the northwest-trending basin axis. In general, strata shallow rapidly toward the basin's western margin (at the rate of 600–1,000 m/km; 1,030–2,040 ft/mi) and shallow gradually through the central and eastern portions of the basin (30–110 m/km; 60–220 ft/mi). Data in the southwestern portion of the PRB show a structural rise along the basin-bounding Casper Arch. The maximum structural relief of Upper Cretaceous strata, measured at the top of the Mowry Shale, is about 4,724 m (15,500 ft) from the deepest part of the basin in Johnson County to outcrop along the eastern margin of the Bighorn Mountains.

Thickness. The majority of the Upper Cretaceous units investigated are thickest in the western or southwestern PRB and thin to the east. In contrast, the Greenhorn, Pool Creek, and Fox Hills are thickest in the southeast and thin to the west. The Mowry is unique in that it is thickest in the northwest and thins to the southeast.

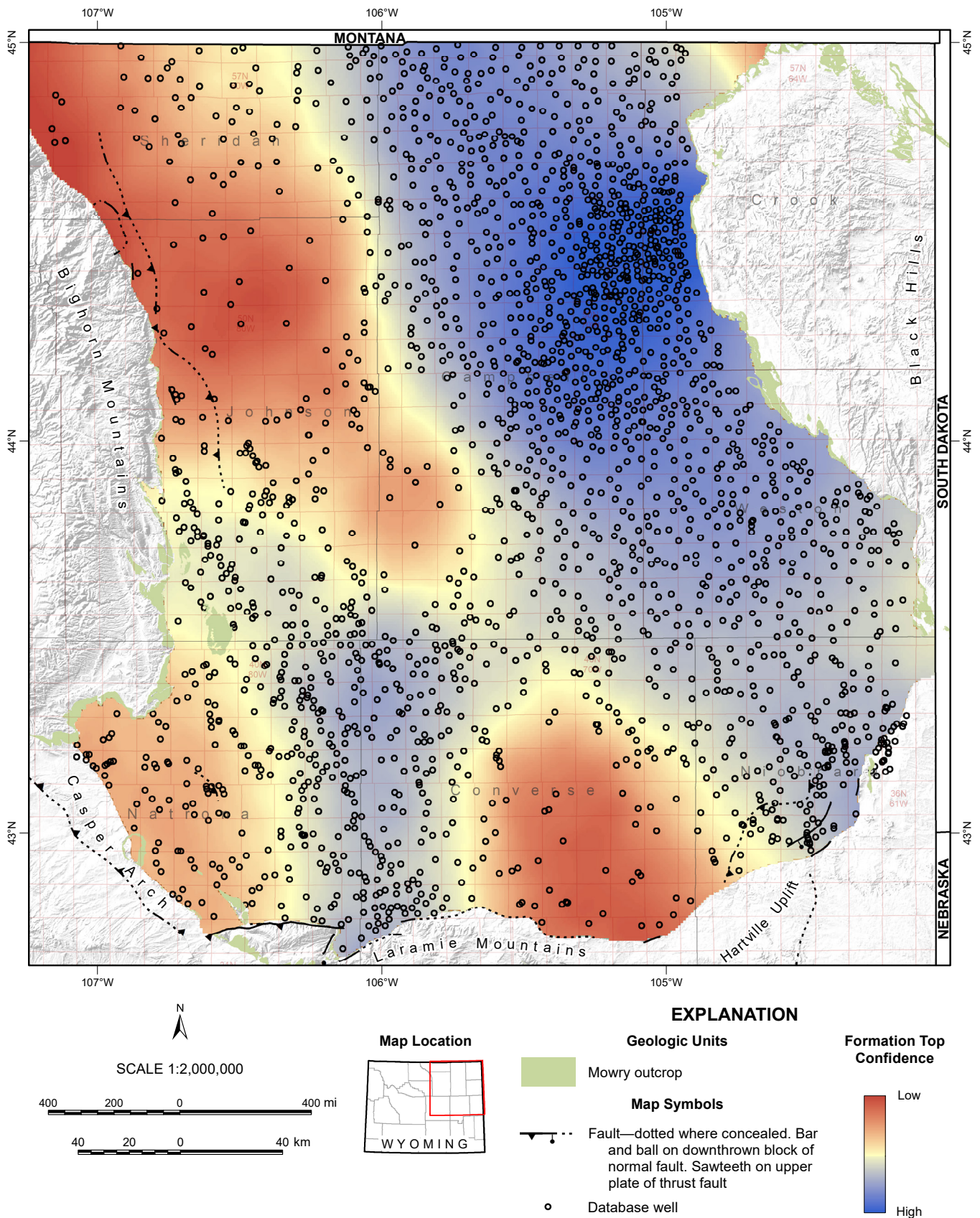


Figure 9. Generalized confidence in contour map predictions, based on average kriging cross validation. The confidence in formation depth where data do not exist depends primarily on data density.

Trends by Formation

Formation tops are reported relative to mean sea level.

Muddy. The top of the Muddy (fig. 10) was observed basin wide and ranges in depth from -2,743 m (-8,999 ft) to 1,673 m (5,489 ft). This study did not interpret the base of the Muddy, so no thickness map was generated.

Mowry. The Mowry was observed throughout the PRB. The top of the Mowry (fig. 11) ranges from -2,648 m (-8,689 ft) to 1,767 m (5,798 ft).

The Mowry and Shell Creek shales were not differentiated. Thickness of the combined shale package (fig. 12) was calculated from the top of the Mowry Shale to the top of the Muddy Sandstone. The combined Mowry and Shell Creek shales are thickest in the northwestern PRB in central Sheridan County, where the combined interval is 134 m (440 ft) thick. The Mowry-Shell Creek interval thins to a minimum of 36 m (119 ft) in west-central Niobrara County. Thinning is rapid from the northwestern portion of the basin toward the basin center (2 m/km; 4 ft/mi) and more gradual from the center to the southeast (0.4 m/km; 0.8 ft/mi).

Belle Fourche. The top of the Belle Fourche (fig. 13) is deepest along the basin axis, with a maximum depth of -2,476 m (-8,124 ft). The shallowest subsurface depth measured for the Belle Fourche was 1,769 m (5,803 ft).

Belle Fourche thickness (fig. 14) was calculated as the difference between the top of the Belle Fourche and the top of the Mowry Shale. The Belle Fourche is thickest in the southwestern PRB, with a maximum thickness of 282 m (926 ft) along the southern margin of the basin in west-central Converse County. In the southeast the Belle Fourche thins to a minimum of 80 m (263 ft) in west-central Niobrara County. Thickness is relatively consistent (150–180 m; 500–600 ft) in a northwest-trending region in the central PRB. To the northeast, the Belle Fourche regains thickness, reaching a local maximum of 223 m (733 ft).

Greenhorn. Greenhorn tops were correlated primarily in the eastern and northern PRB, as the Greenhorn was not observed west of a northwest trend from northeastern Converse County to north-central Johnson County. The Greenhorn top (fig. 15) is deepest in a northwest trend through the center of the PRB, but varies throughout the basin from -2,264 m (-7,428 ft) to 1,236 m (4,054 ft).

Greenhorn thickness (fig. 16) was calculated by subtracting the top of the Belle Fourche from the top of the Greenhorn. The thickness of the Greenhorn is greatest in a north–northeast-trending region in the southeastern PRB, where it reaches a maximum of 113 m (370 ft). The Greenhorn thins to the northwest, with a minimum measured subsurface thickness of 27 m (90 ft) in Sheridan County.

Pool Creek. Observation of the Pool Creek was restricted to the eastern portion of the PRB, as it was not identified southwest of a line trending north-northeast from northwestern Niobrara County to north-central Campbell County. The top of the Pool Creek (fig. 17) is deepest (-1,187 m; -3,895 ft) in southeastern Campbell County. The shallowest Pool Creek measurement was 1,276 m (4,186 ft).

This investigation determined Pool Creek thickness (fig. 18) from the difference between the top of the Pool Creek and the top of the Greenhorn Formation. The Pool Creek is thickest along the eastern margin of the PRB, particularly in the southeast and in the northeast, where it reaches a maximum thickness of 52 m (169 ft). The Pool Creek thins rapidly to the west (approximately 2 m/km; 4 ft/mi). The minimum measured subsurface thickness is 2 m (7.4 ft) in east-central Campbell County.

Turner and Wall Creek. The Wall Creek is found in the western portion of the PRB. It grades into the chronologically equivalent Turner Sandy Member in the eastern PRB, their boundary trending approximately northwest through northeastern Converse County to northern Johnson County (fig. 19). Neither the Wall Creek nor the Turner were observed

northwest of Gillette. The top of the Wall Creek ranges from -2,562 m (-8,082 ft) to 1,676 m (5,498 ft). The top of the Turner is deepest (-1,795 m; -5,890 ft) in the central PRB, at its boundary with the Wall Creek. The shallowest Turner top measured was 1,151 m (3,775 ft).

The thickness of the Wall Creek (fig. 20) is the difference in subsea depth between the top of the Wall Creek and the top of the Belle Fourche Member of the Frontier Formation. The Wall Creek is thickest in the southwestern PRB, with a maximum thickness of 95 m (311 ft) in east-central Natrona County, near Casper. From this location the Wall Creek thins in all directions. North of the Johnson-Natrona County line, the Wall Creek thins rapidly and is not observed north of Buffalo. Turner thickness was calculated as the difference between the top of the Turner and either the top of the Pool Creek Member of the Carlile Shale or the top of the Greenhorn Formation. In Converse and Niobrara counties, the Turner maintains a consistent thickness of approximately 37–43 m (120–140 ft). The Turner is thickest in Weston County, at the western basin margin (88 m; 289 ft), but thins to 40 m (120 ft) northwest of the Weston-Crook County line at the Wyoming-Montana border.

Sage Breaks and Carlile. The top of the combined Sage Breaks-Carlile surface (fig. 21) ranges from -2,363 m (-7,753 ft) to 1,722 m (5,650 ft).

The thickness of the combined Sage Breaks-Carlile interval was not calculated due to variations in nomenclature and age throughout the basin (Lynds and Slattery, 2017). However, the thickness of the Sage Breaks in the eastern PRB was calculated as the difference between the top of the Sage Breaks and the top of the Turner (fig. 22). The Sage Breaks is thickest (213 m; 699 ft) along the eastern margin of the PRB, in northwestern Crook County. In general the Sage Breaks thins to the west and southwest. The thickness decreases locally in an elongate northwest-trending region in northeastern Converse County and southern Campbell County, where a minimum subsurface thickness of 47 m (153 ft) was observed. This trend agrees with that of the scour at the base of the Niobrara described by Weimer and Flexer (1985).

Niobrara. Along the basin axis in east-central Converse County, the top of the Niobrara (fig. 23) is deepest at -2,219 m (-7,280 ft). The shallowest Niobrara measurement was east of the Casper Arch in central Natrona County (1,628 m; 5,341 ft).

The thickness of the Niobrara (fig. 24) is the difference between the top of the Niobrara and either the Sage Breaks or Carlile. The maximum thickness of the Niobrara (284 m; 931 ft) is in the southwestern PRB in the vicinity of the Casper Arch. The Niobrara thins to the northeast, to its outcrop along the eastern margin of the PRB. The minimum subsurface thickness observed was 23 m (74 ft) in north-central Campbell County. Thickness increases locally in eastern Converse County, reaching a maximum of about 207 m (680 ft).

Shannon. The extent of the Shannon is limited to the western PRB and was not observed east of a line trending north-northwest from western Converse County to northwestern Campbell County. The Shannon is deepest (-1,873 m; -6,146 ft) in a northwest-trending region near the basin axis (fig. 25). The Shannon is shallowest (1,667 m; 5,469 ft) near the southwestern basin margin, and also gradually shallows to the north toward the Wyoming-Montana border.

The Shannon is thickest (fig. 26) in west-central Converse County (68 m; 223 ft). To the north the Shannon thins rapidly (1.3 m/km; 2.6 ft/mi) to central Johnson County, north of which it thins gradually (0.2 m/km; 0.3 ft/mi), with a minimum observed subsurface thickness of 4 m (13 ft) near the Wyoming-Montana border.

Sussex. Observation of the Sussex was limited to the southwestern and central PRB. The Sussex was not identified in the southeastern PRB nor north of the Johnson-Sheridan County line. The top of the Sussex (fig. 27) ranges from -1,692 m (-5,551 ft) to 1,481 m (4,860 ft).

The Sussex is thickest (fig. 28) in a northwest-trending region in northwestern Converse County (35 m; 115 ft). The Sussex thins rapidly to both the southwest and northeast (about 1.6 m/km; 3.2 ft/mi). Measured subsurface thickness is a minimum of 5 m (15 ft) in eastern Natrona County as well as in west-central Campbell County.

Red Bird Silty and Parkman. The Parkman is located primarily in the western PRB. It grades into the Red Bird in the eastern PRB. The approximate boundary between the Red Bird and Parkman trends north-northwest, subparallel to the basin axis, through central Converse County to northeastern Campbell County. The Parkman-Red Bird interval follows general basin trends (fig. 29), with the Parkman reaching its maximum depth along the basin axis (-1,462 m; -4,797 ft). The shallowest Parkman top measured was 1,560 m (5,117 ft). As the Parkman grades into the Red Bird, the interval shallows gradually toward the eastern margin of the PRB.

The thickness of the Parkman is simply the difference between its top and base, whereas the thickness of the Red Bird is the difference between its top and the top of the Mitten Shale (fig. 30). The Parkman is thickest in the southwestern PRB, with a maximum measured thickness of 223 m (733 ft) at the southern margin of the PRB in west-central Converse County. The Parkman thins to the northeast as it grades into the Red Bird east of the approximate Parkman-Red Bird boundary line, and continues to thin to the northeastern portion of the basin. The maximum observed subsurface thickness of the Red Bird is 185 m (606 ft) in the southeastern PRB in western Niobrara County, and the minimum observed is 15 m (49 ft) at the Wyoming-Montana border in northeastern Campbell County.

Teapot. The top of the Teapot (fig. 31) is deepest along the basin axis (-1,379 m; -4,522 ft). The shallowest top measured for the Teapot Sandstone was 1,628 m (5,342 ft). Although the Teapot is formally a member of the Mesaverde Formation, a correlative sandstone was observed within the Pierre Shale in the southeastern PRB, and is considered the Teapot Sandstone in this study.

The thickness of the Teapot (fig. 32) is greatest along the basin axis in the western PRB, with a maximum thickness of 54 m (176 ft) in south-central Sheridan County. Northeast of a northwest-trending line from western Niobrara County to eastern Sheridan County, the Teapot thins rapidly (1.1 m/km; 2.1 ft/mi) and is absent in the northeastern and east-central PRB.

Teckla. Identification of the Teckla was limited to the southwestern and west-central PRB. The top of the Teckla (fig. 33) is deepest in Johnson County (-1,260 m; -4,135 ft) and shallowest in northeastern Natrona County (1,677 m; 5,503 ft). Although the Teckla is formally a member of the Lewis Shale, a correlative sandstone was observed within the Pierre Shale in the southeastern PRB, and is considered the Teckla Sandstone in this study.

The Teckla is thickest (fig. 34) in the southern and southwestern PRB, reaching its maximum thickness of 96 m (316 ft) at the southern margin of the basin in southeastern Converse County. The Teckla thins to the north (1.0 m/km; 2.0 ft/mi), and is not observed north of the Johnson-Sheridan County line. The Teckla thins rapidly (5.7 m/km; 11 ft/mi) along a northwest-trending line from western Niobrara County to northeastern Johnson County, and is absent in the northeastern and east-central PRB.

Fox Hills. The Fox Hills was observed throughout the PRB. The base of the Fox Hills is the top of the combined Bearpaw, Pierre, and Lewis surface (fig. 35), which is deepest along the basin axis (-1,220 m; -4,001 ft) and shallowest along the basin's western margin (1,638 m; 5,375 ft). The top of the Fox Hills (fig. 36) is deepest in a northwest-trending region through east-central Johnson County (-1,180 m; -3,871 ft). The shallowest Fox Hills top identified was 1,623 m (5,325 ft).

The thickness of the Fox Hills is the difference between its top and the top of either the Lewis, Pierre, or Bearpaw shales. The subsurface thickness of the Fox Hills (fig. 37) is generally greatest in the southeastern and southwestern PRB, with a maximum of 136 m (445 ft) in south-central Weston County. The Fox Hills thins to the northwest (1.8 m/km; 3.5 ft/mi), with a minimum observed subsurface thickness of 15 m (48 ft) in northwestern Campbell County.

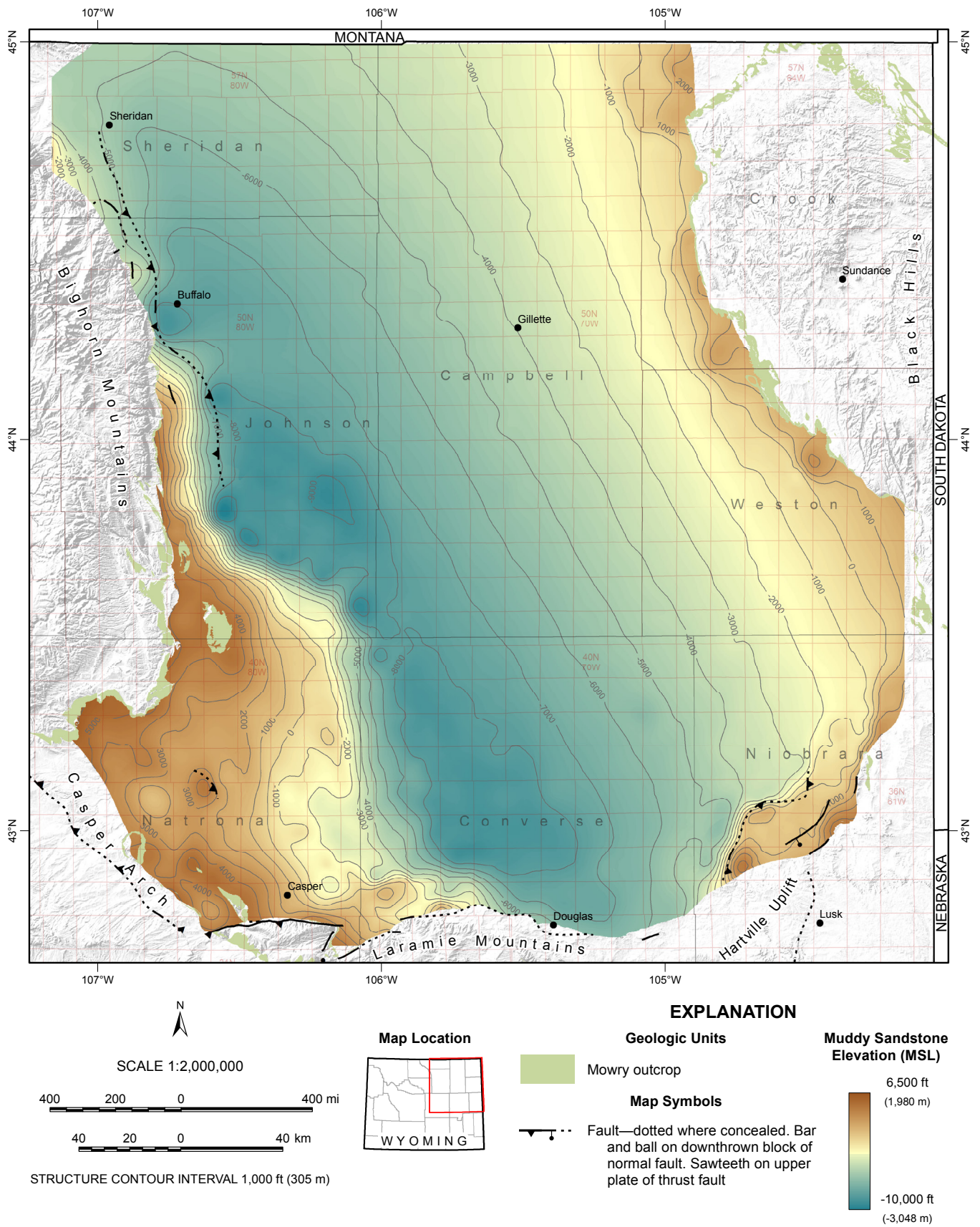


Figure 10. Structure map of top of the Muddy Sandstone. Elevation is relative to mean sea level (MSL).

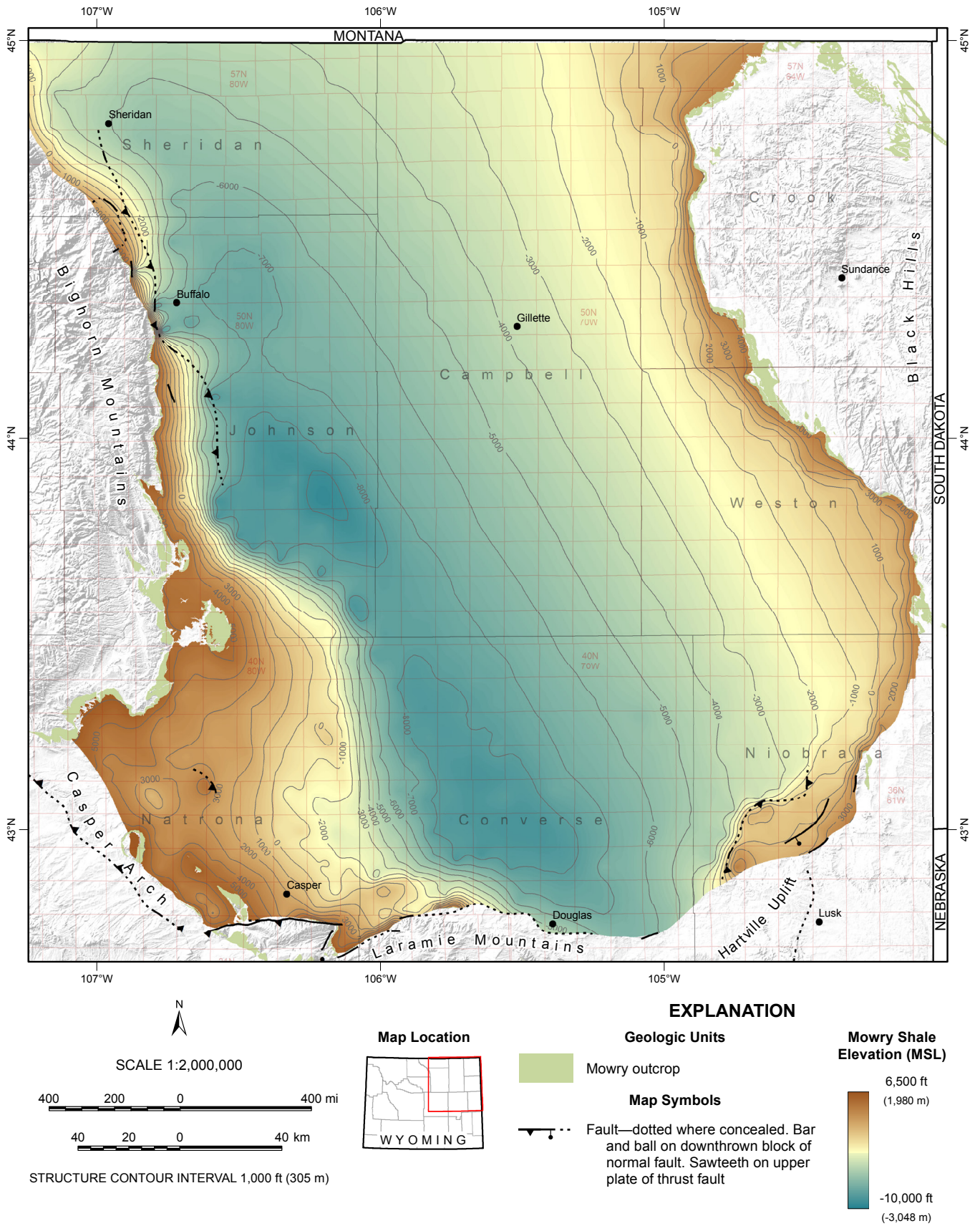


Figure 11. Structure map of top of the Mowry Shale. Elevation is relative to mean sea level (MSL).

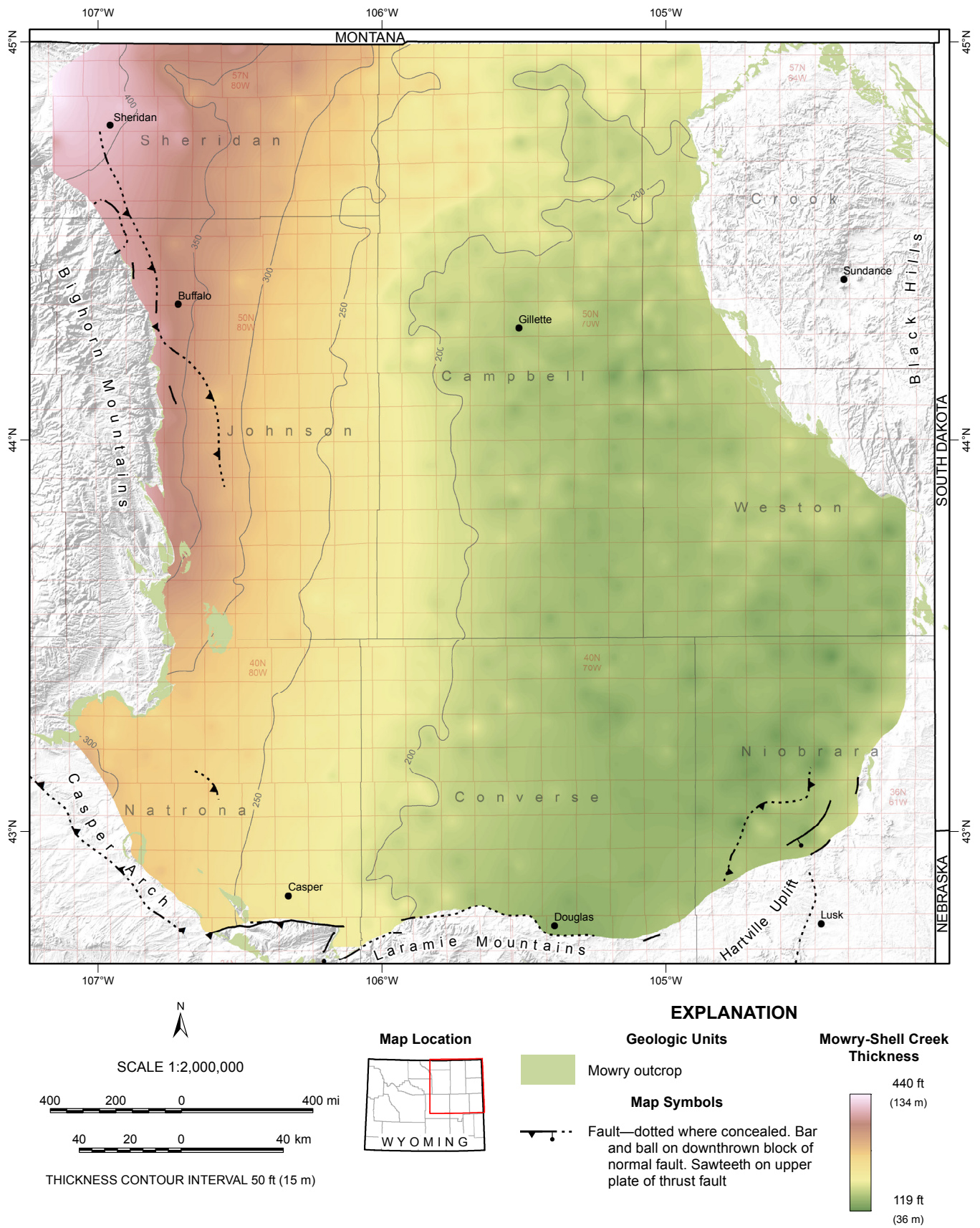


Figure 12. Thickness of the combined Mowry Shale-Shell Creek Shale interval.

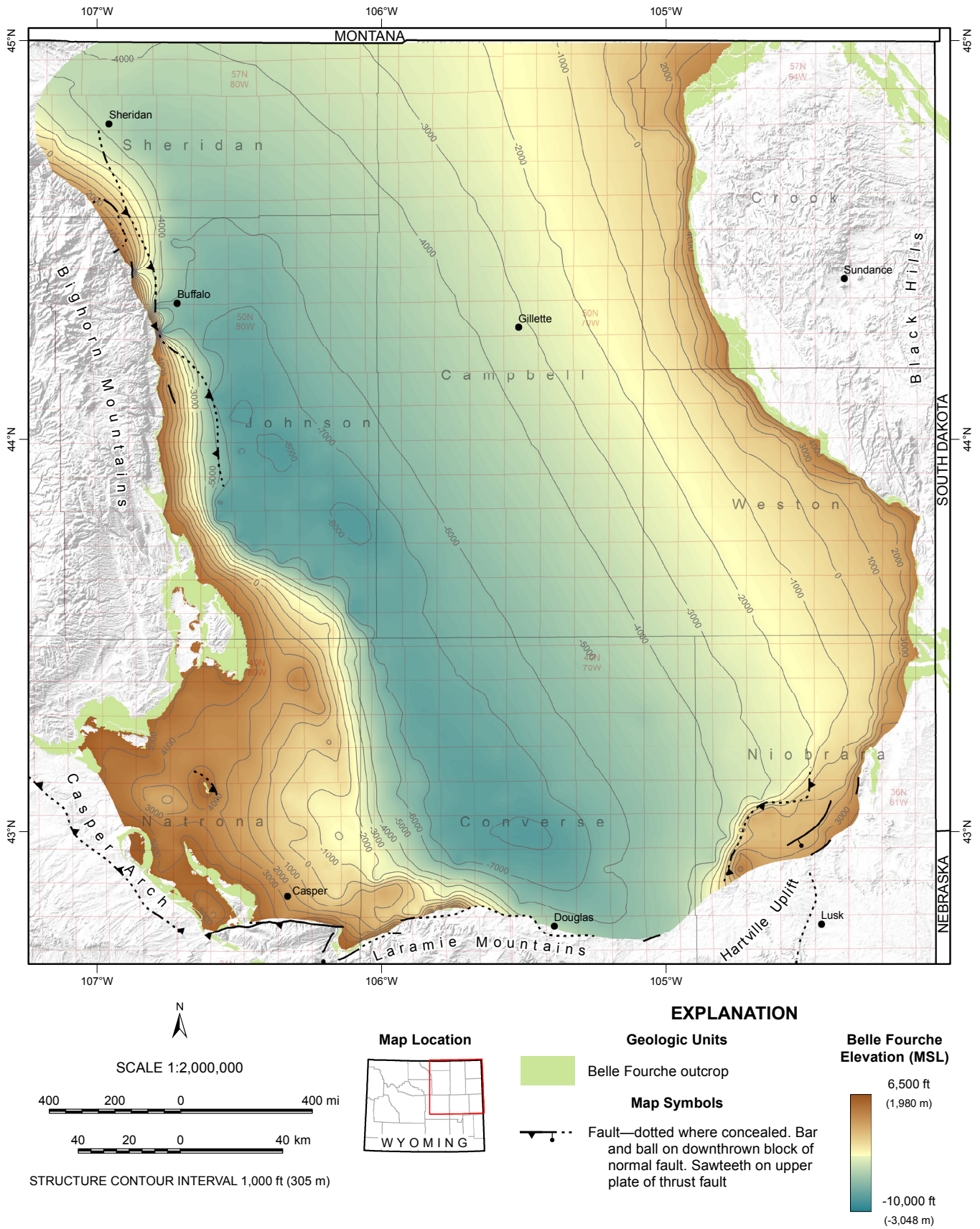


Figure 13. Structure map of top of the Belle Fourche Formation, or Belle Fourche Member of the Frontier Formation. Elevation is relative to mean sea level (MSL).

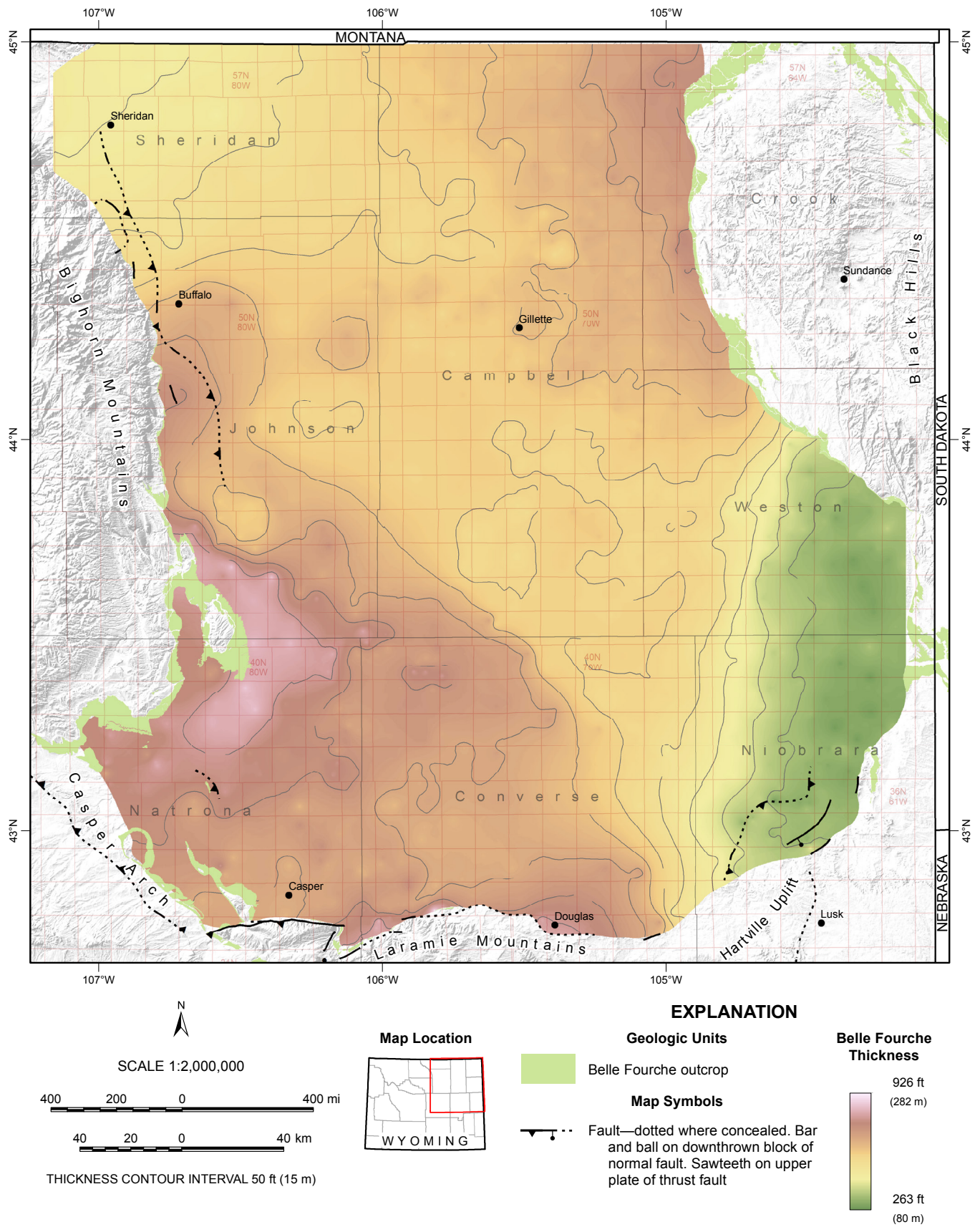


Figure 14. Thickness of the Belle Fourche Formation, or Belle Fourche Member of the Frontier Formation.

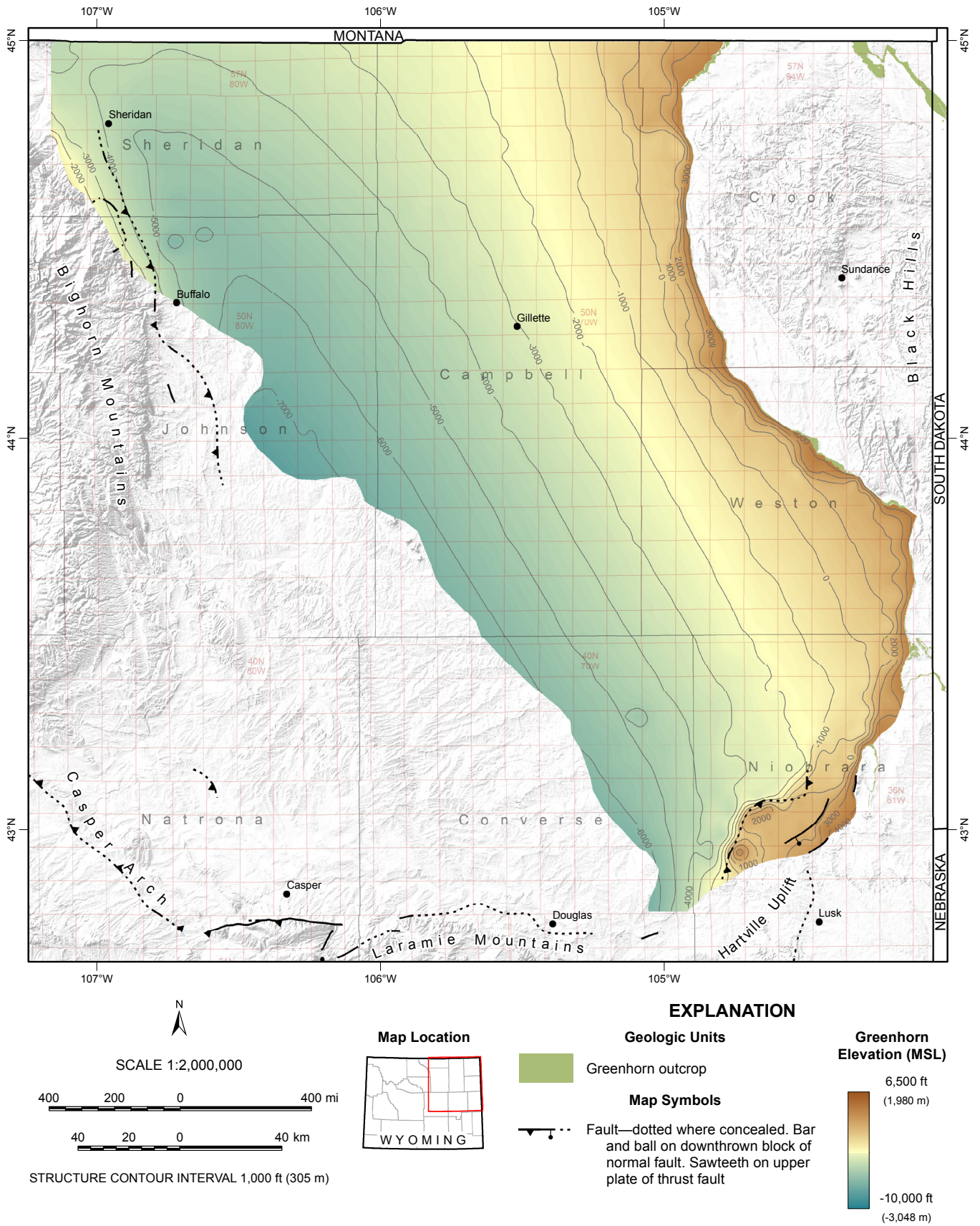


Figure 15. Structure map of top of the Greenhorn Formation. Elevation is relative to mean sea level (MSL).

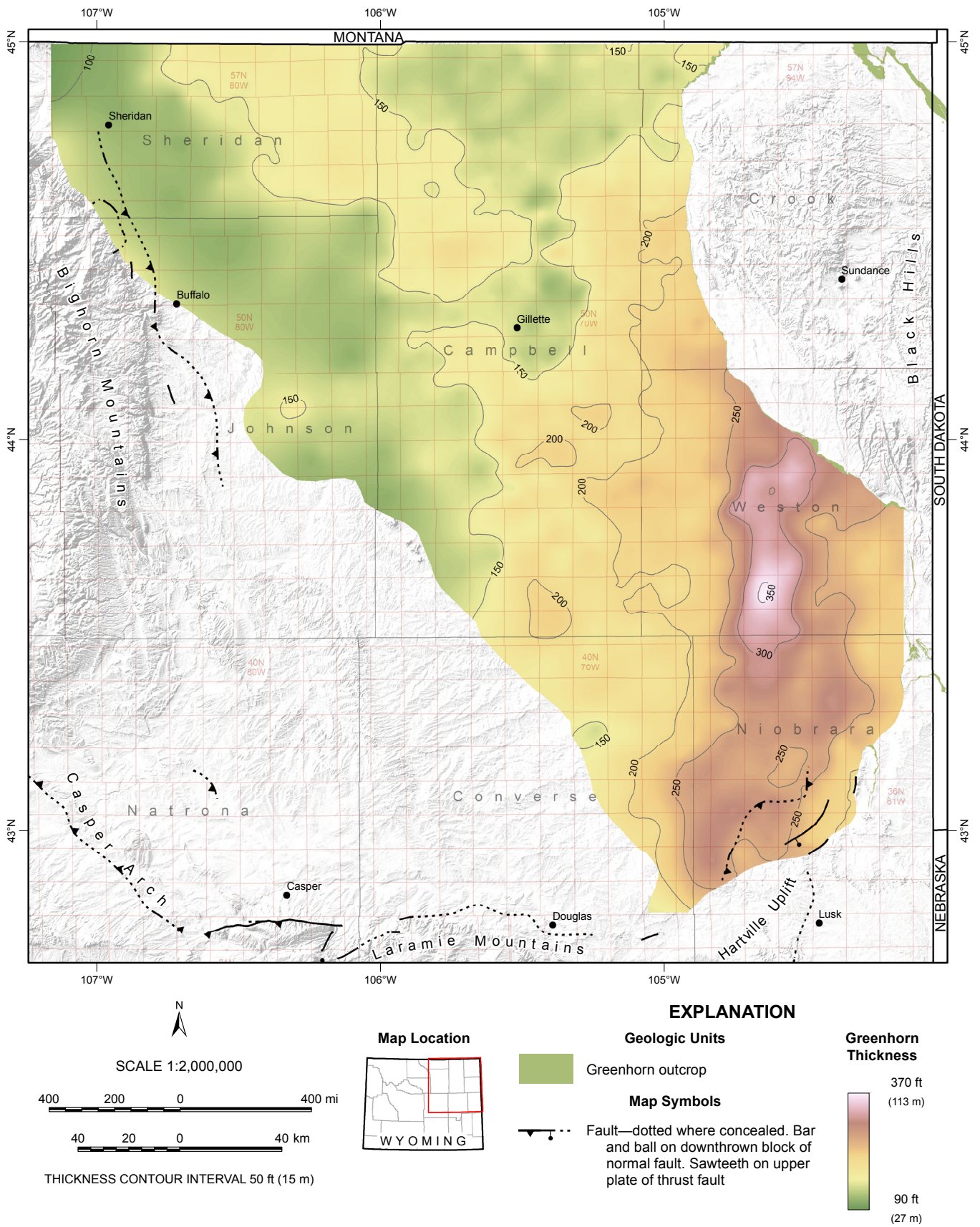


Figure 16. Thickness of the Greenhorn Formation.

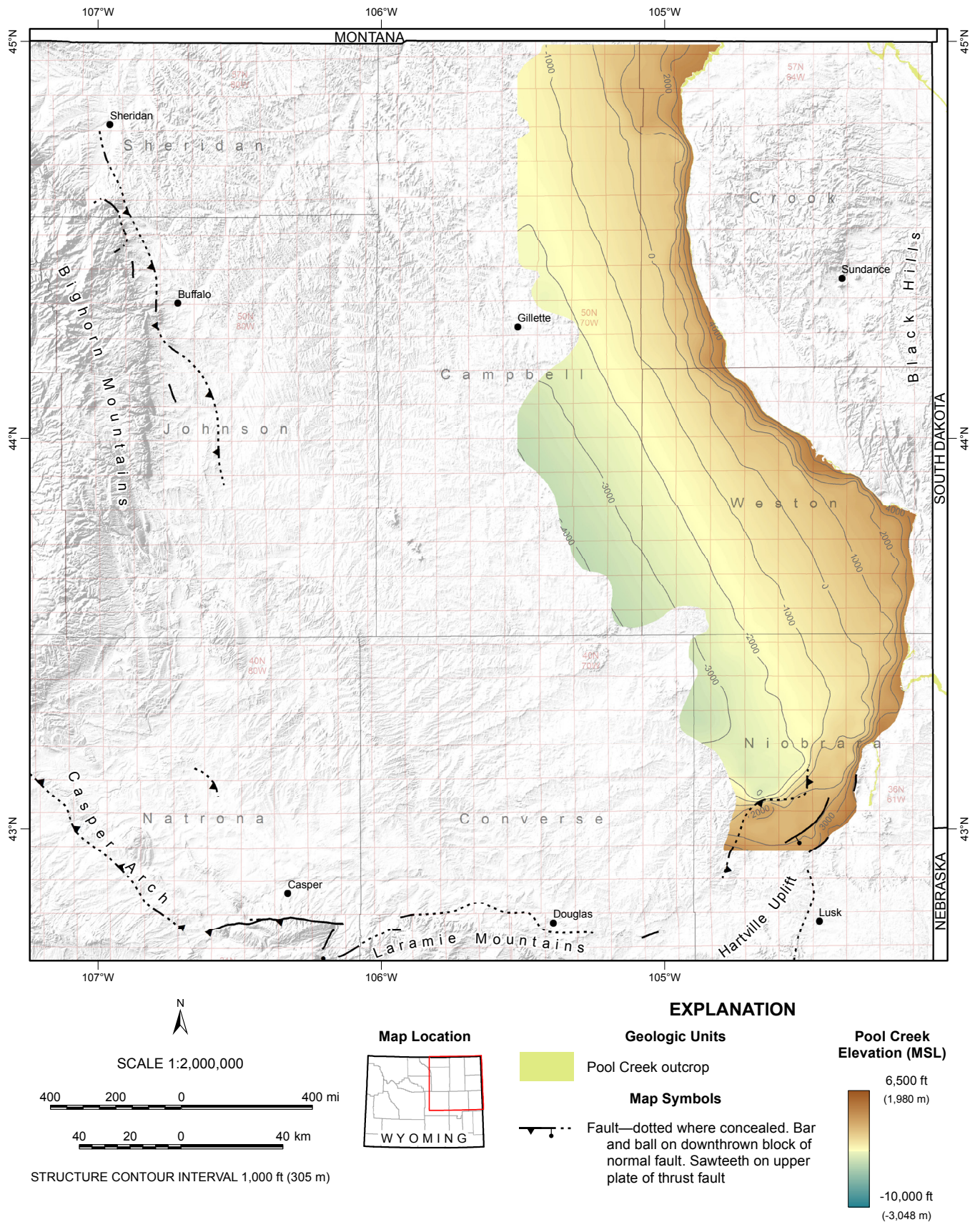


Figure 17. Structure map of top of the Pool Creek Member of the Carlile Shale. Elevation is relative to mean sea level (MSL).

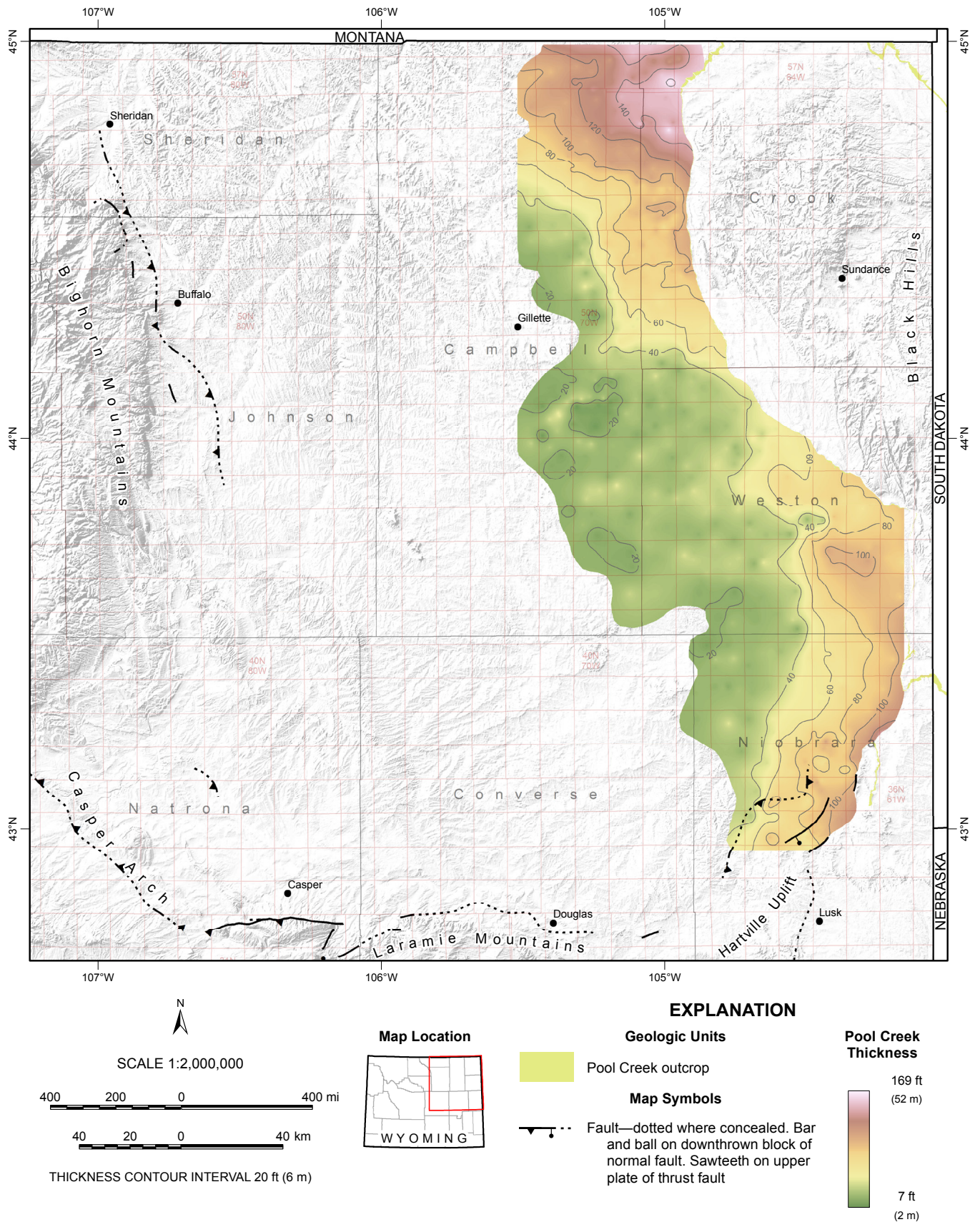


Figure 18. Thickness of the Pool Creek Member of the Carlile Shale.

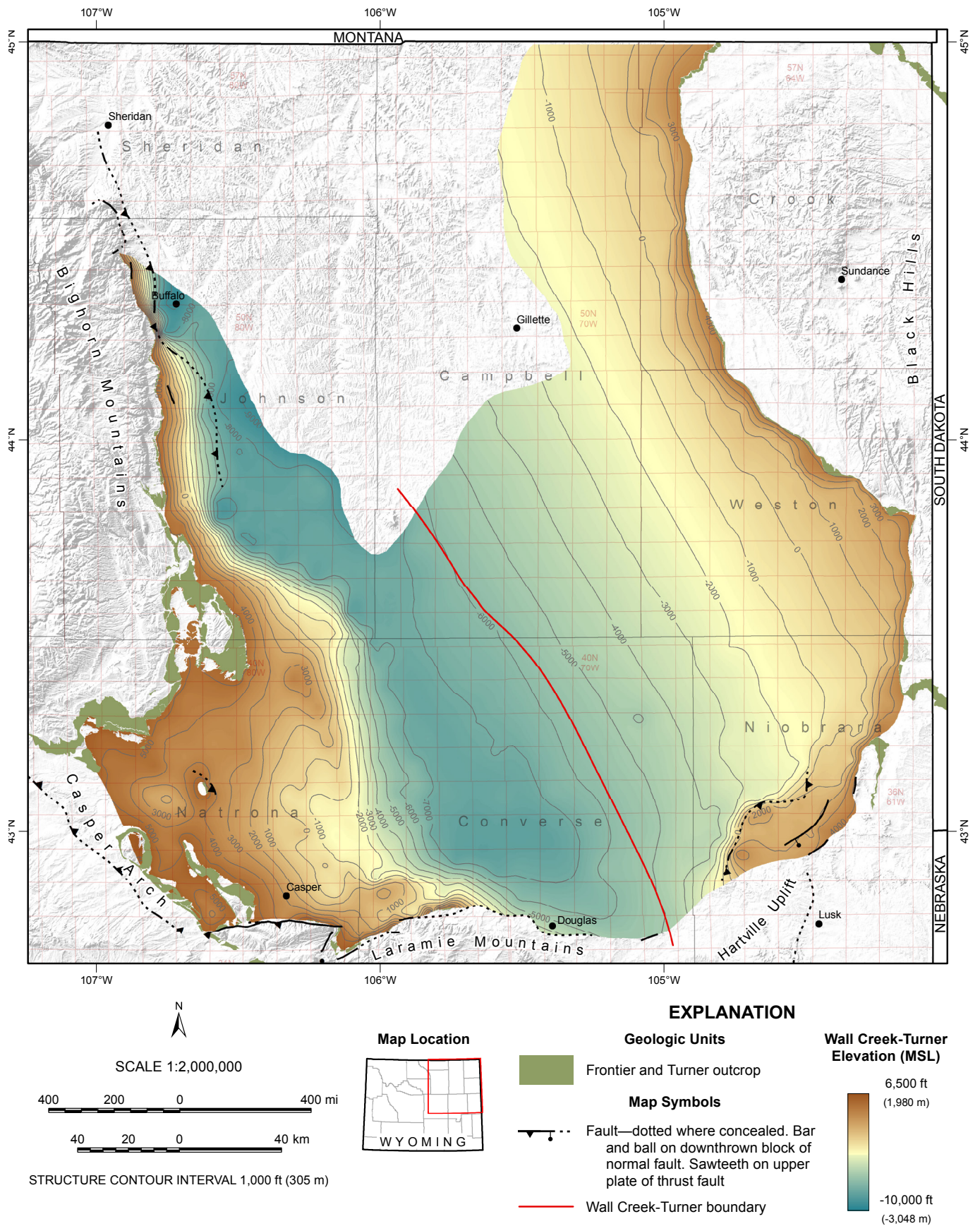


Figure 19. Structure map of top of the combined Turner Sandy Member of the Carlile Shale and Wall Creek Member of the Frontier Formation. Elevation is relative to mean sea level (MSL).

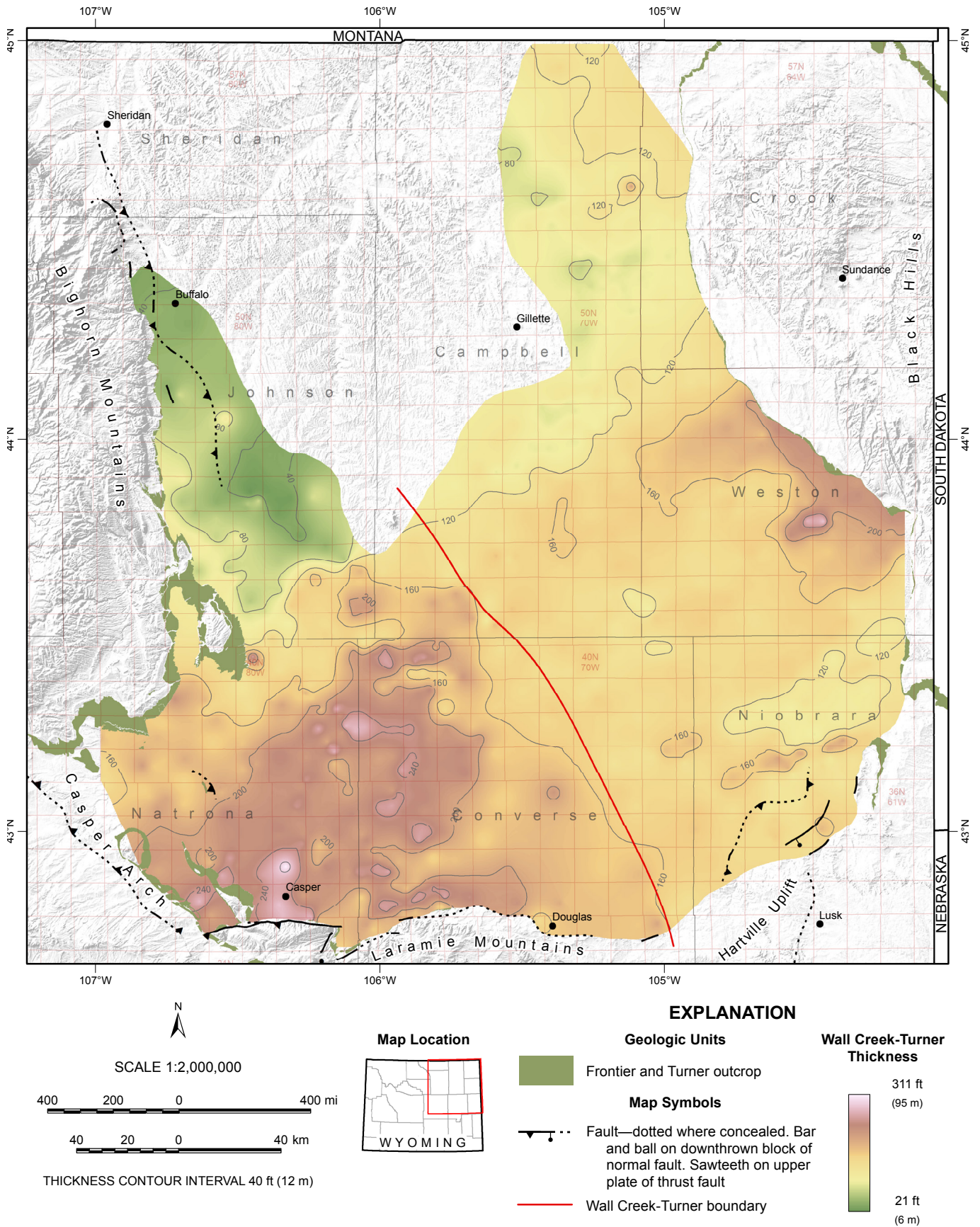


Figure 20. Thickness of the combined Turner Sandy Member of the Carlile Shale and Wall Creek Member of the Frontier Formation.

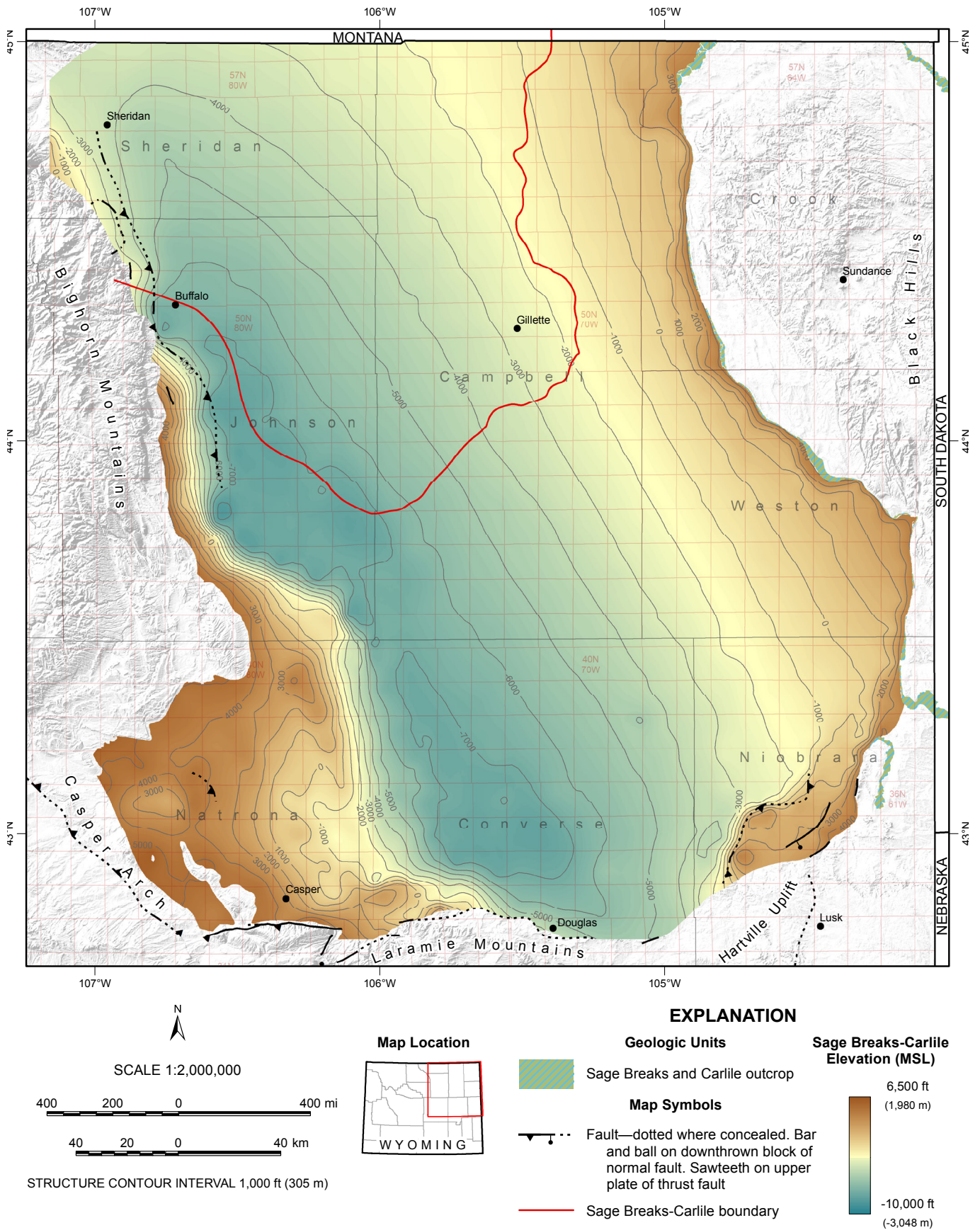


Figure 21. Structure map of top of the combined Sage Breaks Member of the Carlile or Cody shales and Carlile Member of the Cody Shale. Elevation is relative to mean sea level (MSL).

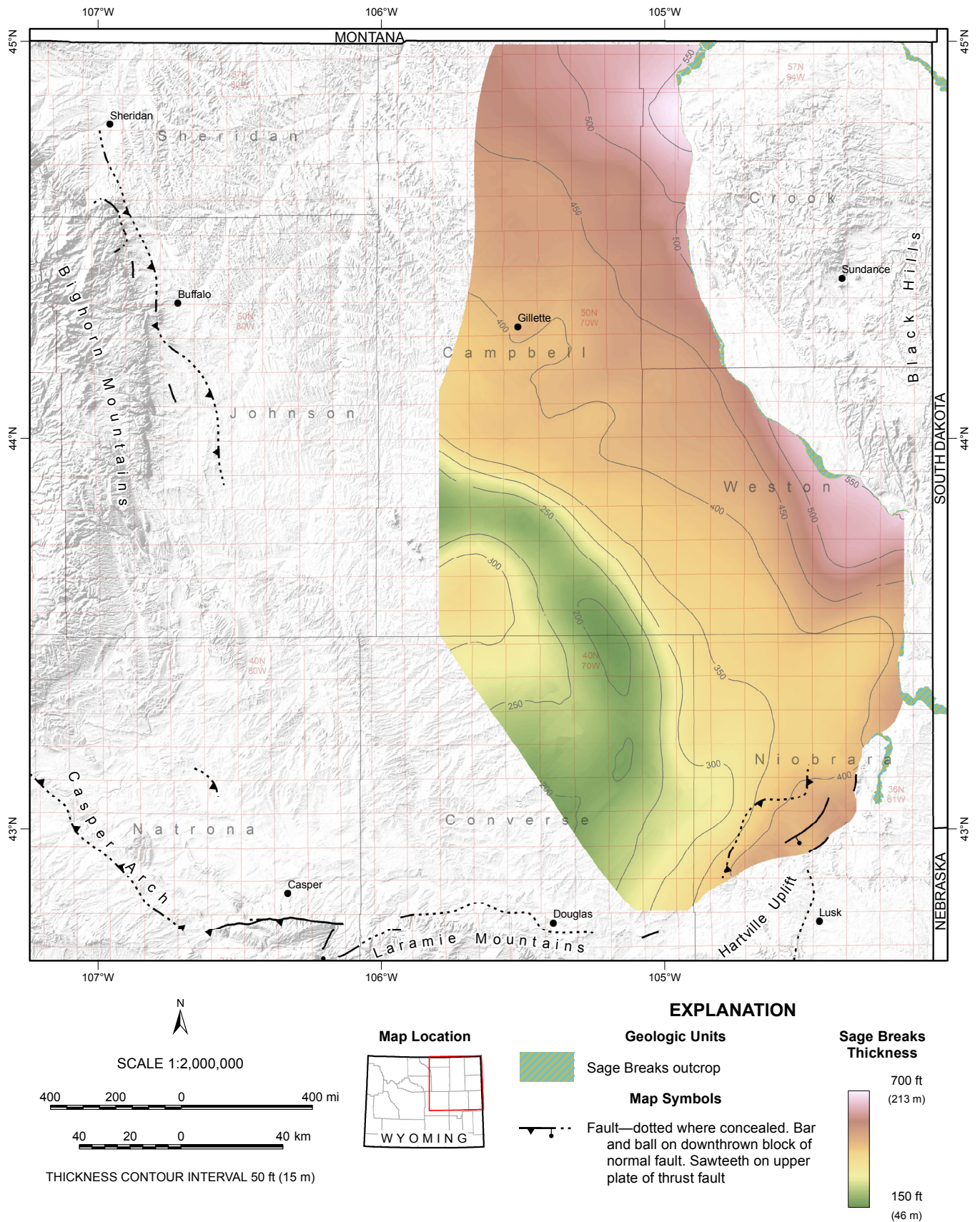


Figure 22. Thickness of the Sage Breaks Member of the Carlile Shale.

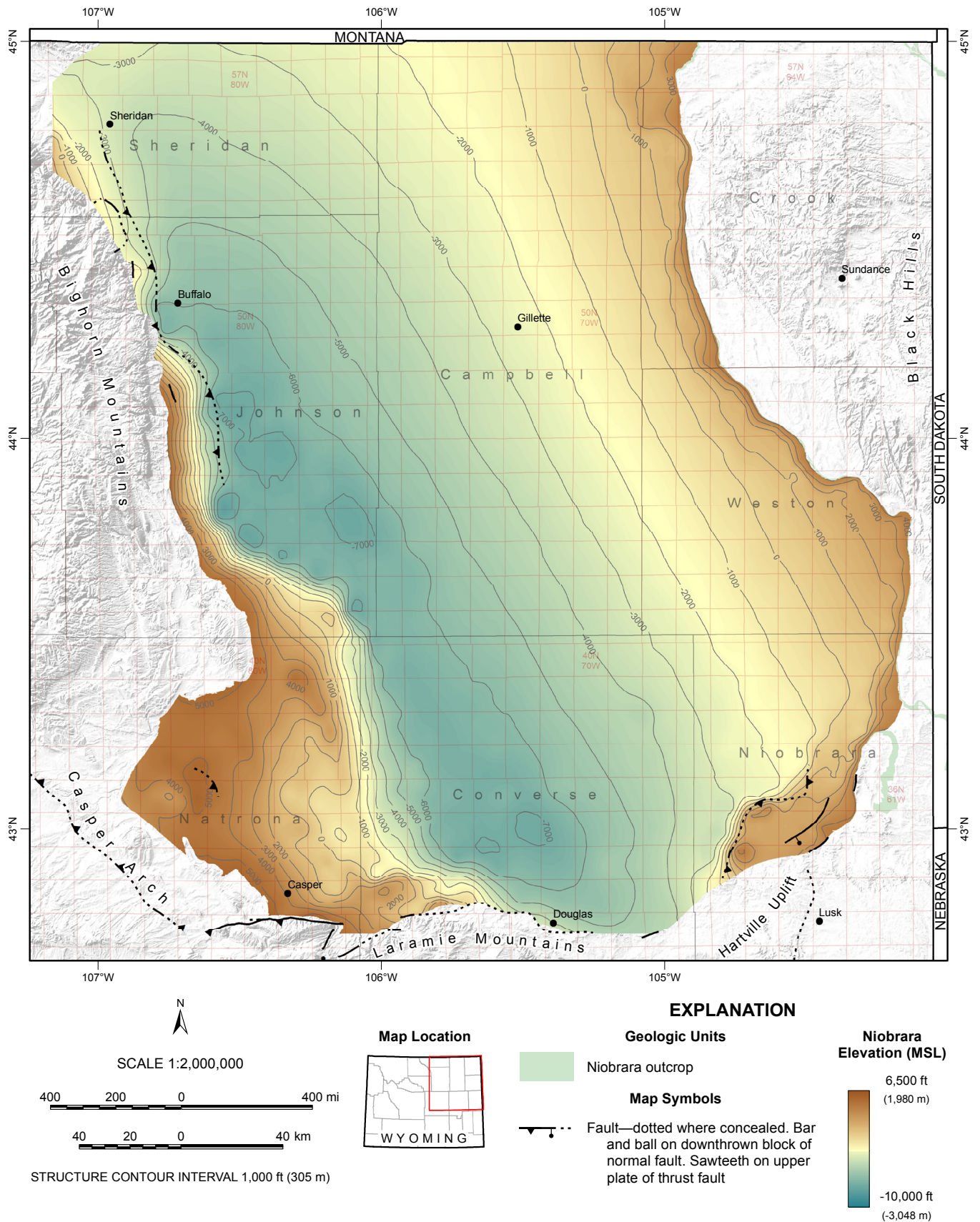


Figure 23. Structure map of top of the Niobrara Formation or Niobrara Member of the Cody Shale. Elevation is relative to mean sea level (MSL).

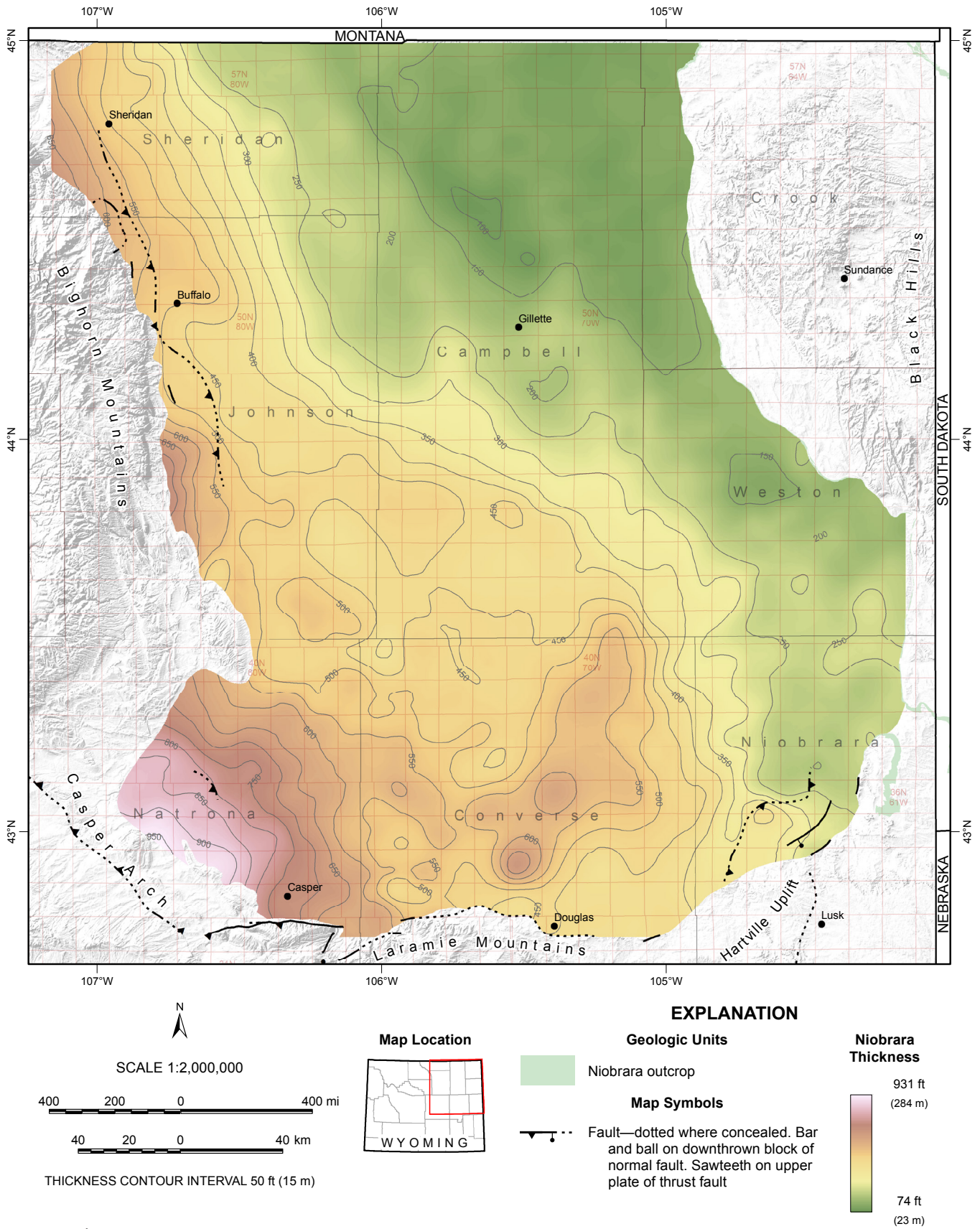


Figure 24. Thickness of the Niobrara Formation or Niobrara Member of the Cody Shale.

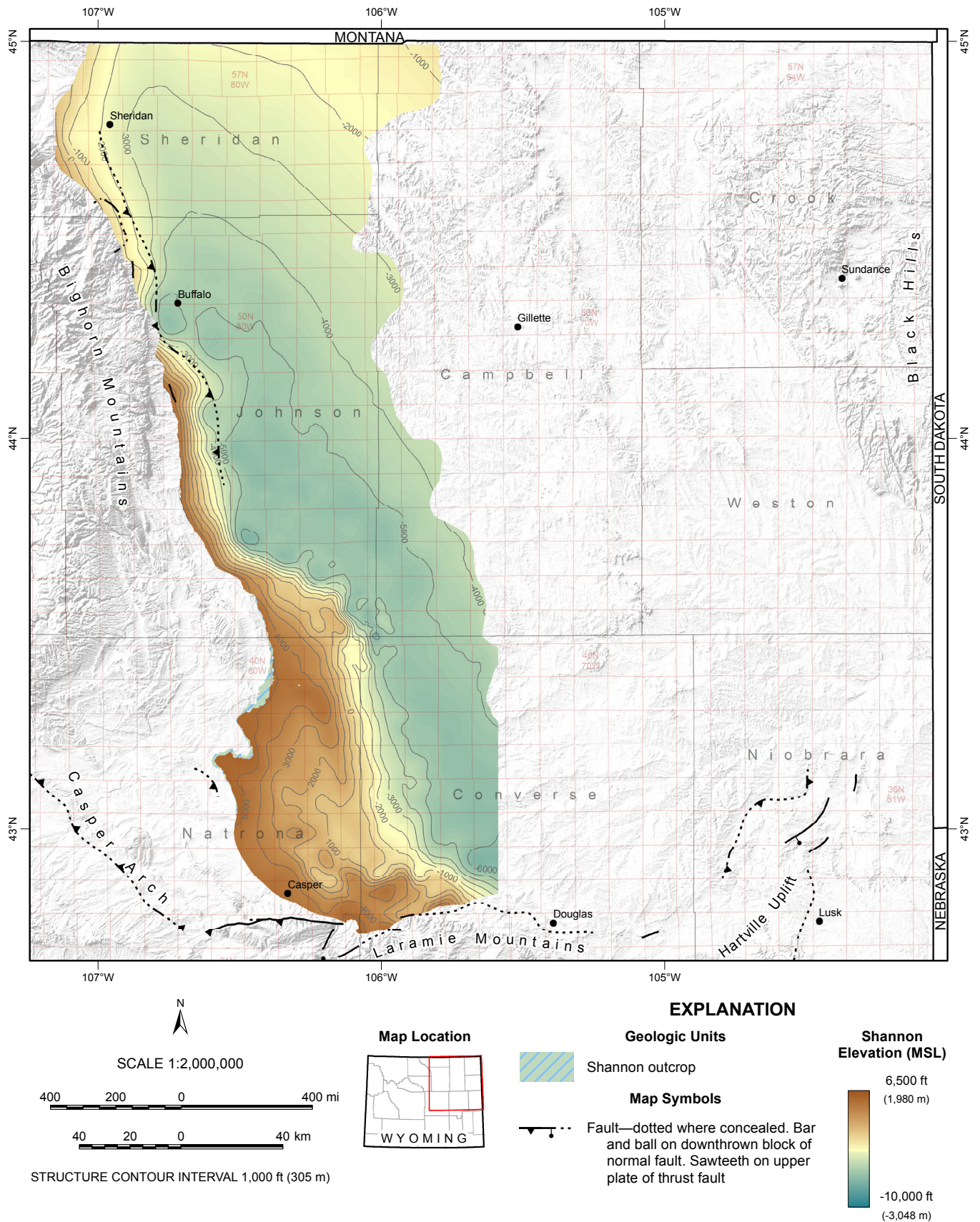


Figure 25. Structure map of top of the Shannon Sandstone Member of the Cody Shale. Elevation is relative to mean sea level (MSL).

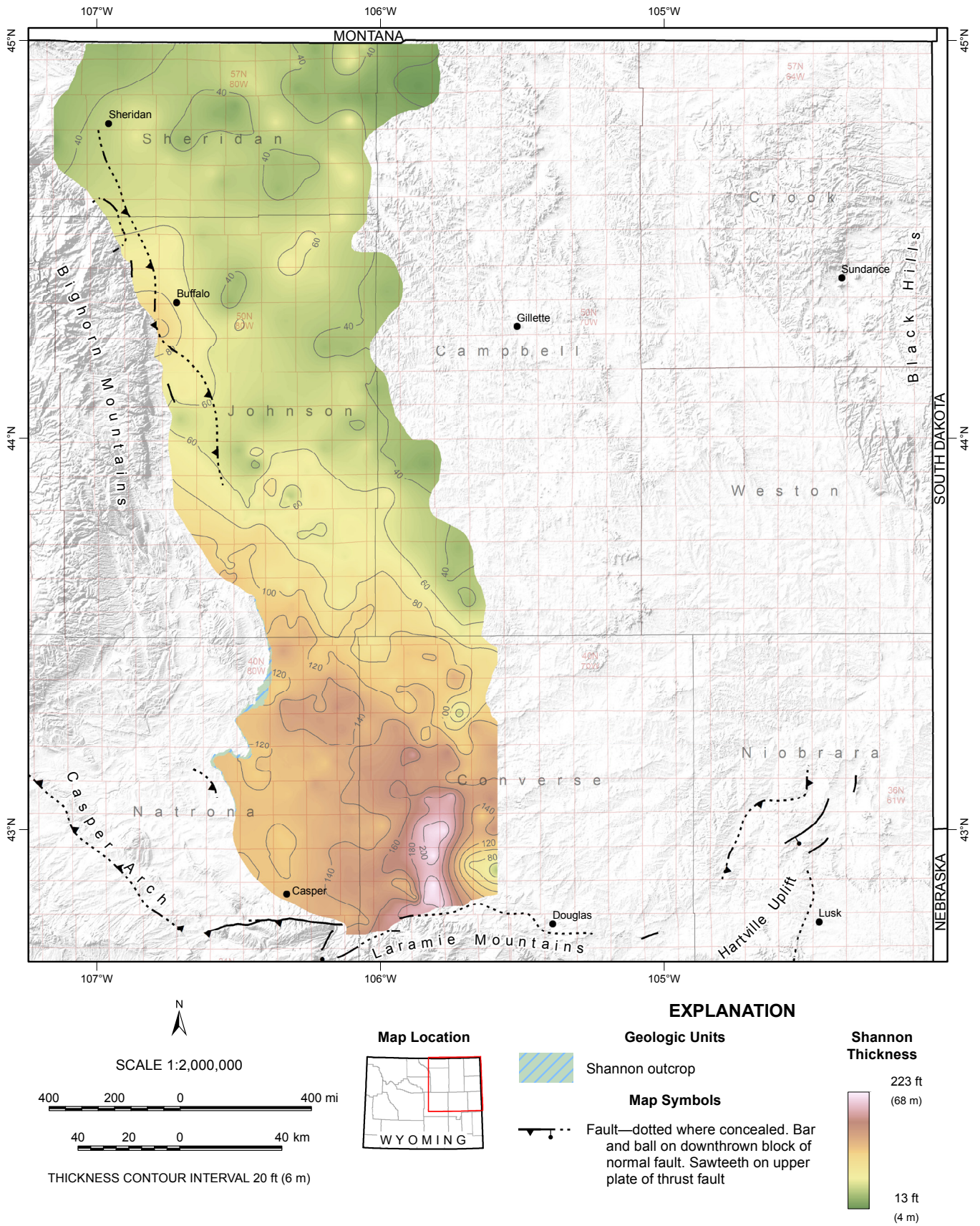


Figure 26. Thickness of the Shannon Sandstone Member of the Cody Shale.

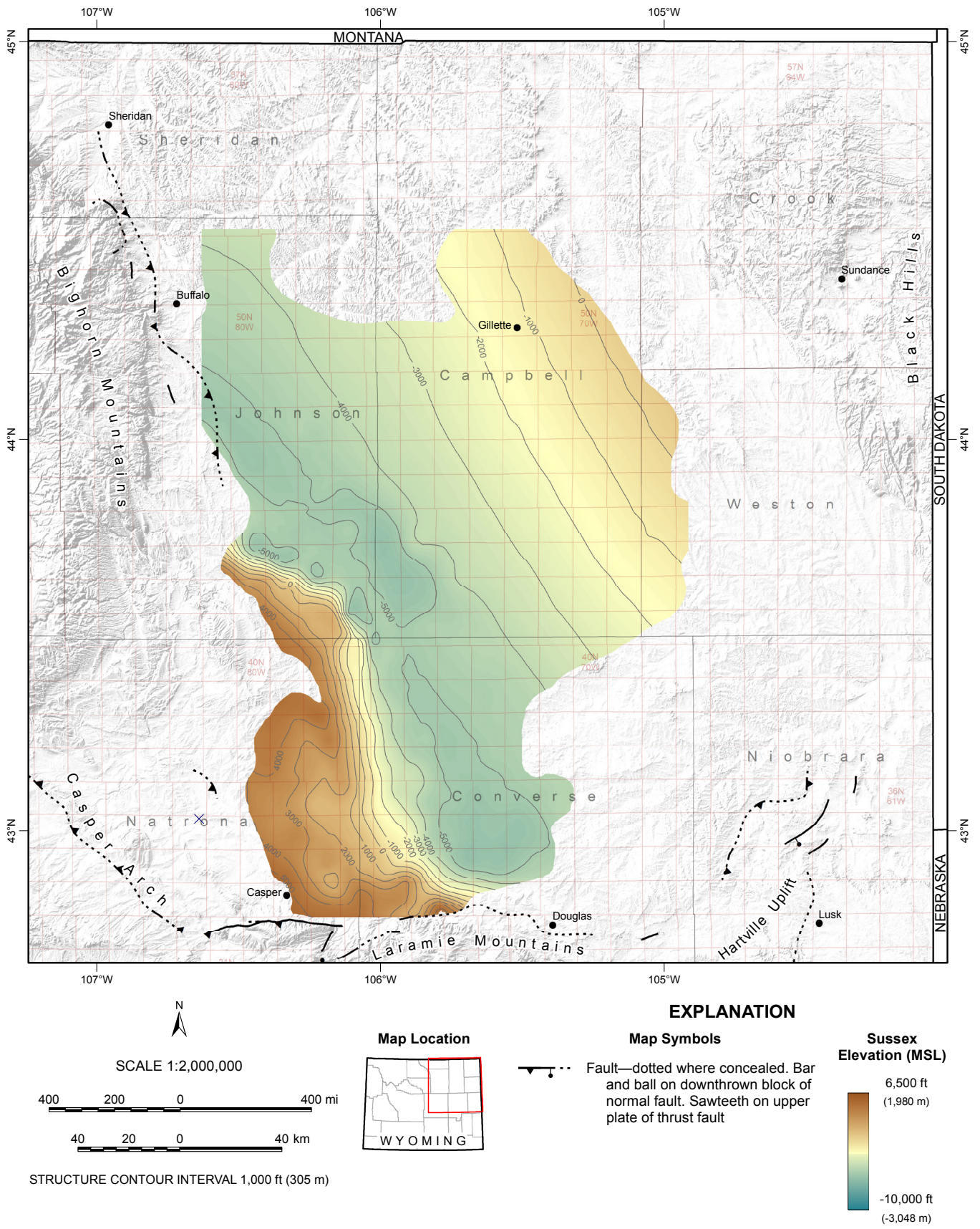


Figure 27. Structure map of top of the Sussex Sandstone Member of the Cody Shale. Elevation is relative to mean sea level (MSL).

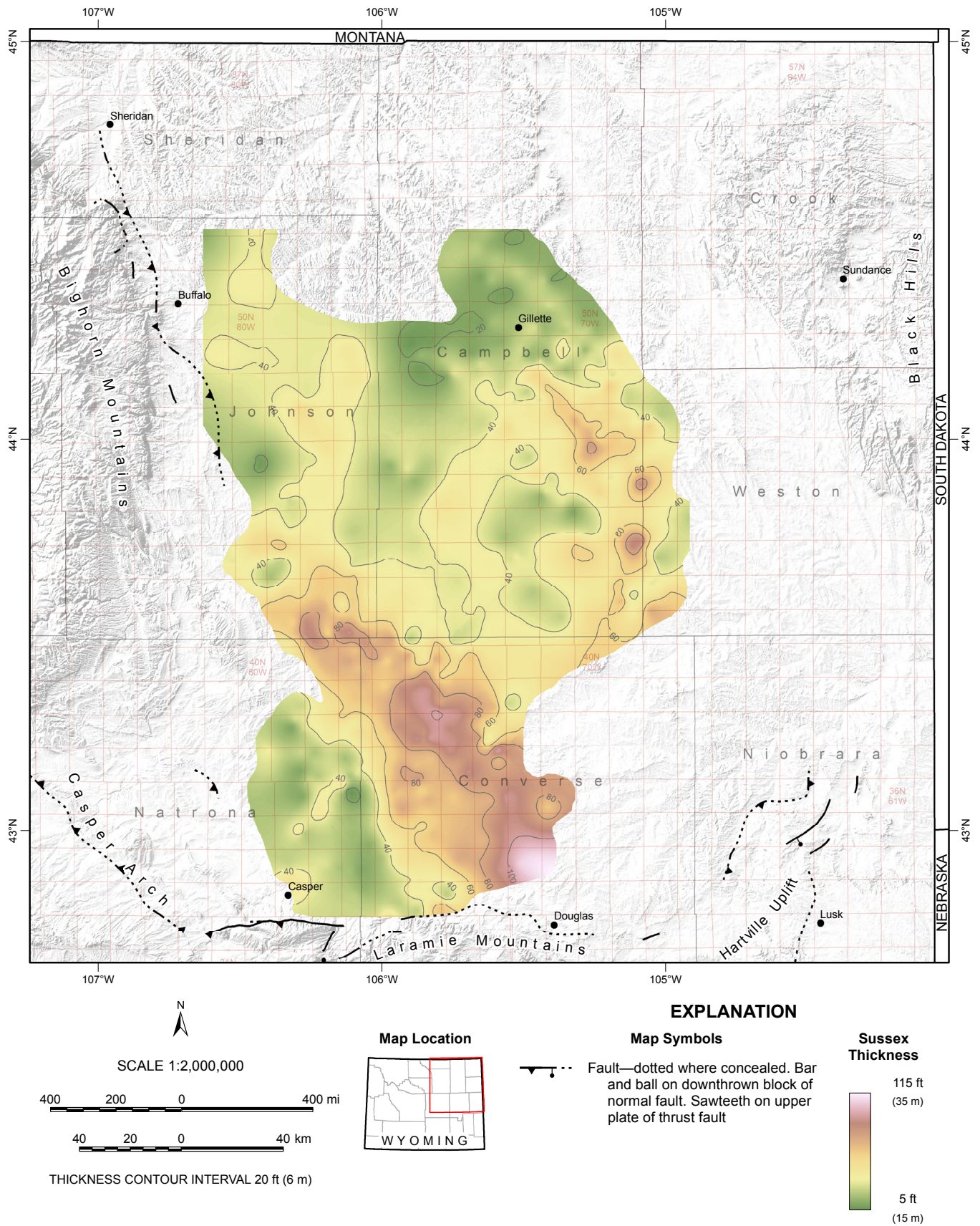
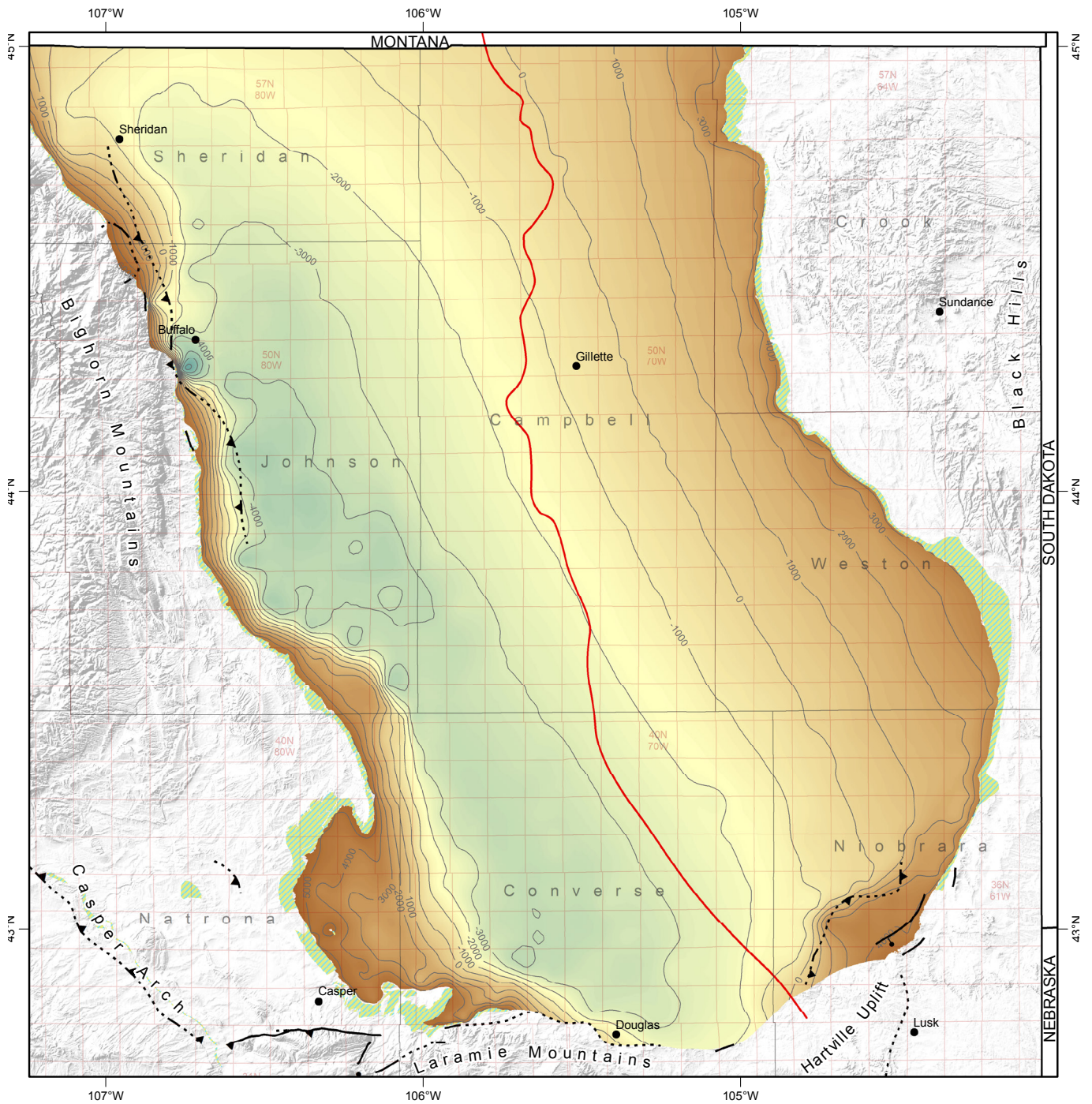


Figure 28. Thickness of the Sussex Sandstone Member of the Cody Shale.



EXPLANATION

Geologic Units

- Parkman and Red Bird outcrop

Map Symbols

- Fault—dotted where concealed. Bar and ball on downthrown block of normal fault. Sawteeth on upper plate of thrust fault
- Parkman-Red Bird boundary

Parkman-Red Bird Elevation (MSL)

- 6,500 ft (1,980 m)
- 10,000 ft (-3,048 m)

Map Location

WYOMING

SCALE 1:2,000,000

400 200 0 400 mi

40 20 0 40 km

STRUCTURE CONTOUR INTERVAL 1,000 ft (305 m)

Figure 29. Structure map of top of the combined Red Bird Silty Member of the Pierre Shale and Parkman Sandstone Member of the Mesaverde Formation. Elevation is relative to mean sea level (MSL).

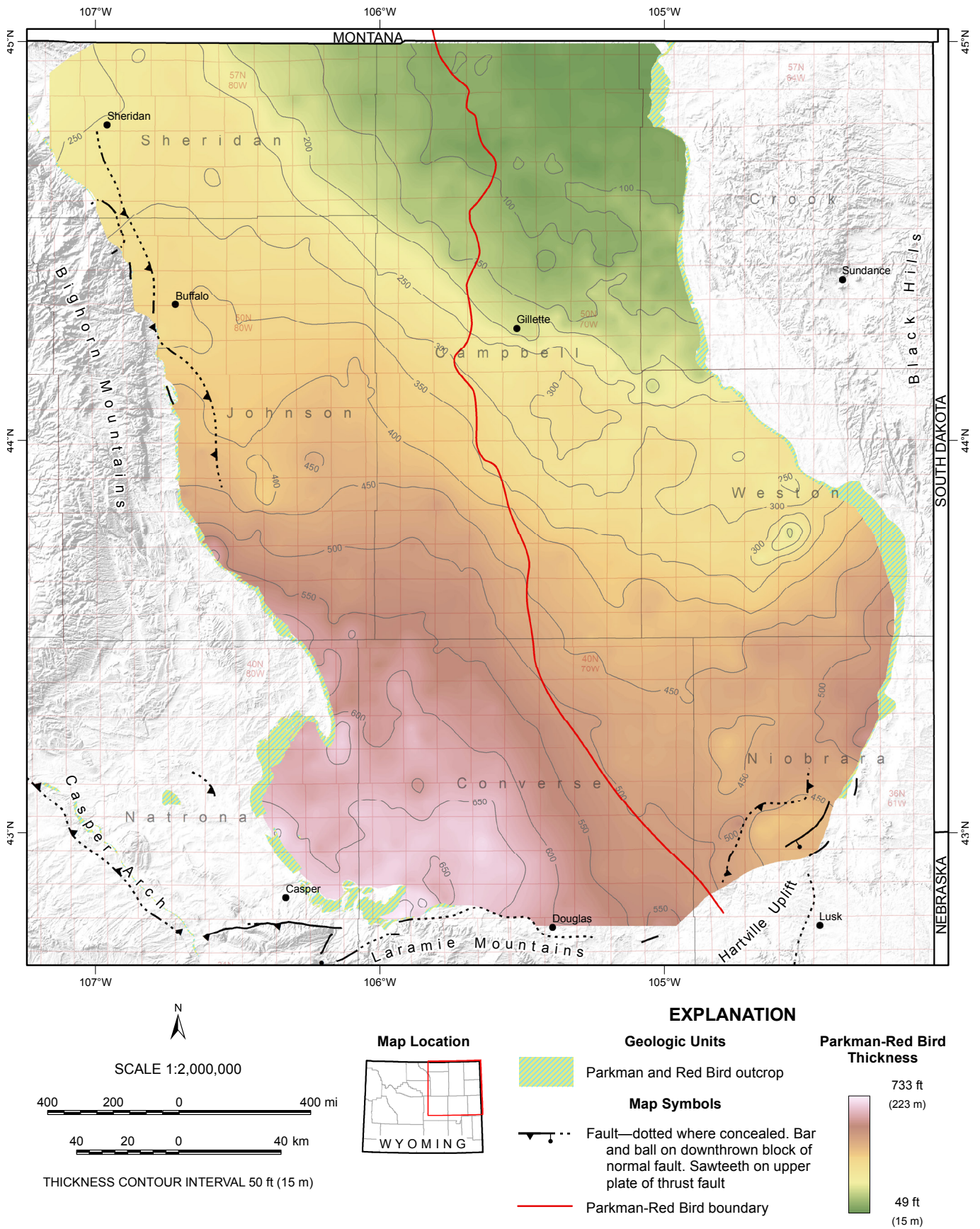


Figure 30. Thickness of the combined Red Bird Silty Member of the Pierre Shale and Parkman Sandstone Member of the Mesaverde Formation.

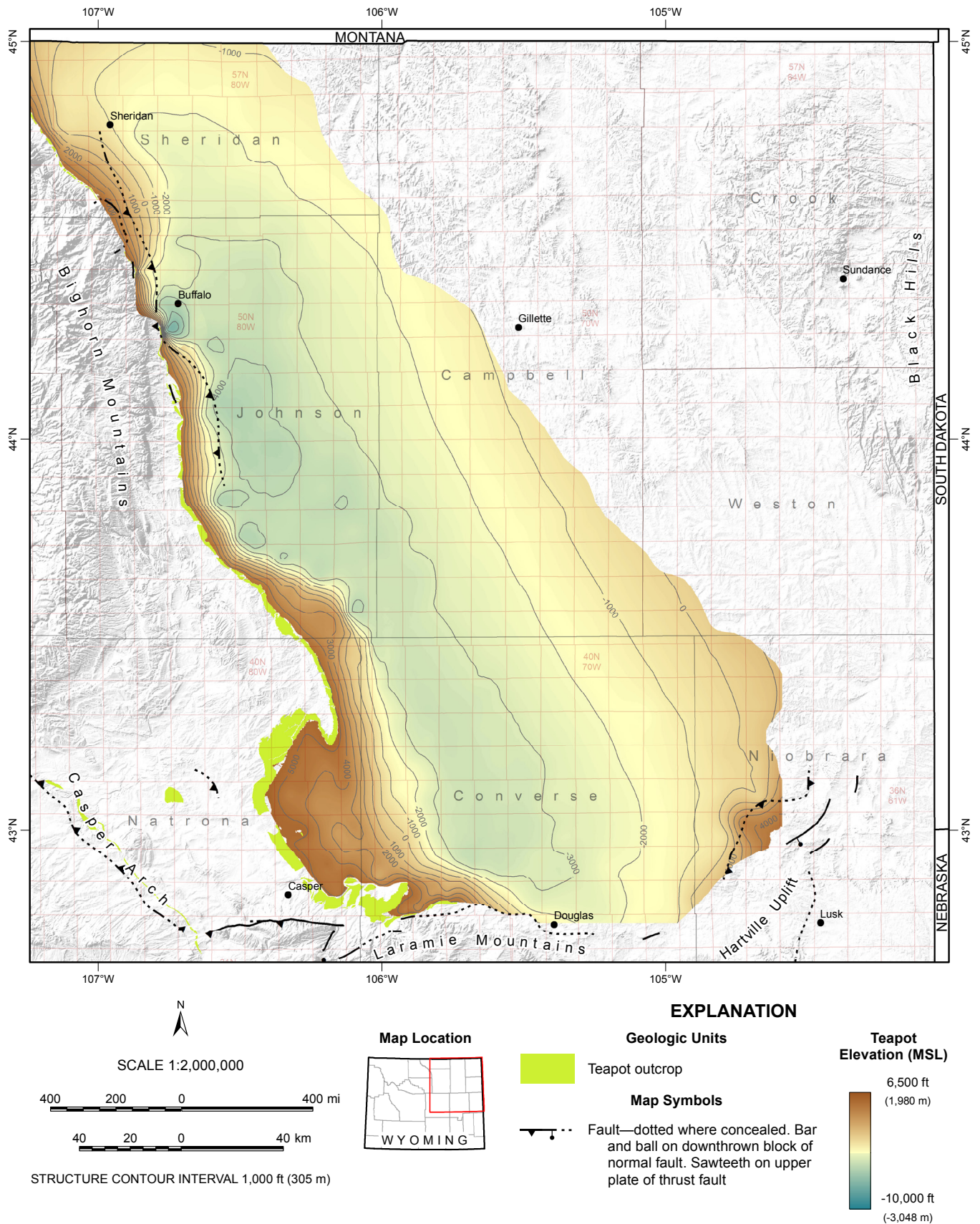


Figure 31. Structure map of top of the Teapot Sandstone Member of the Mesaverde Formation. Elevation is relative to mean sea level (MSL).

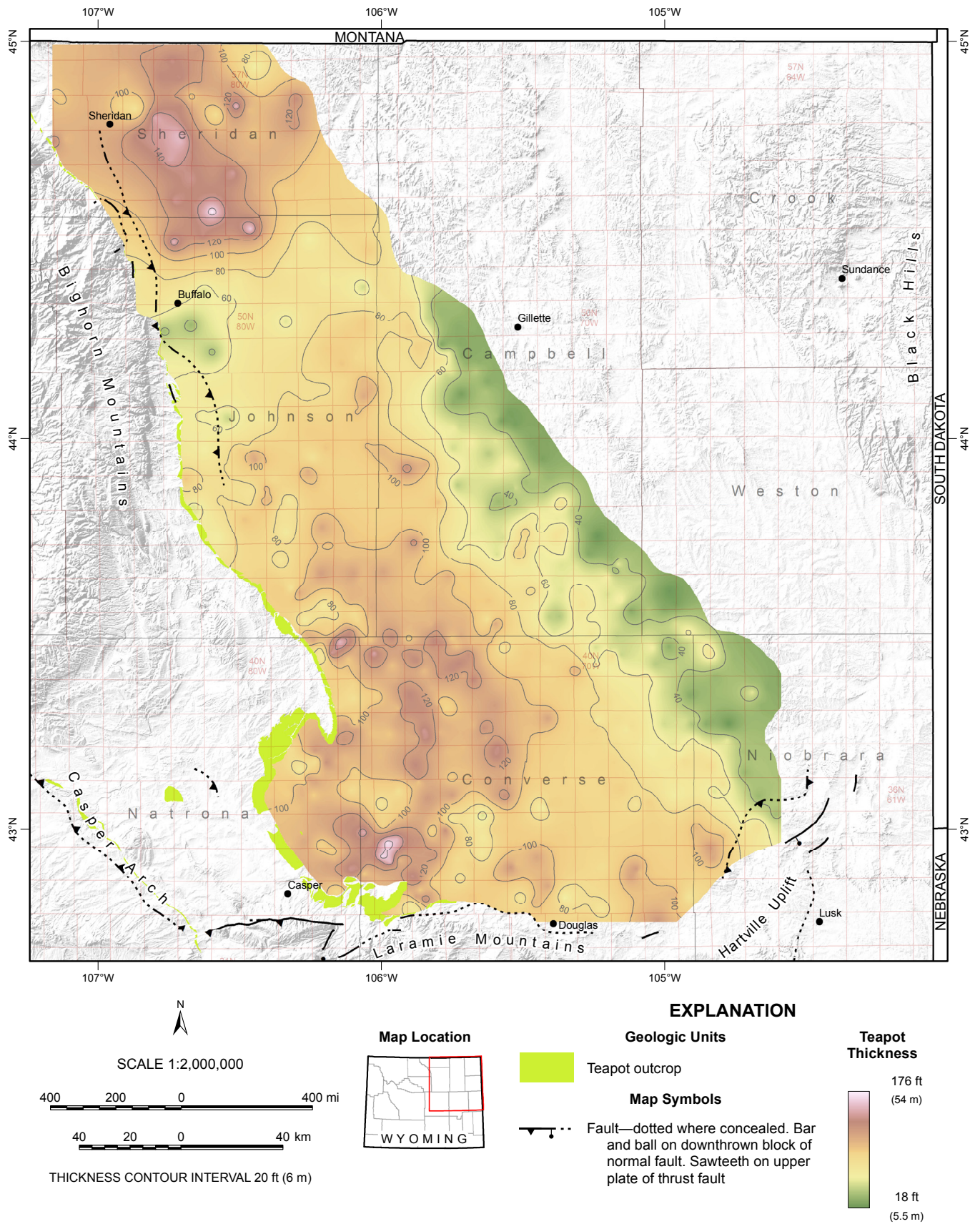


Figure 32. Thickness of the Teapot Sandstone Member of the Mesaverde Formation.

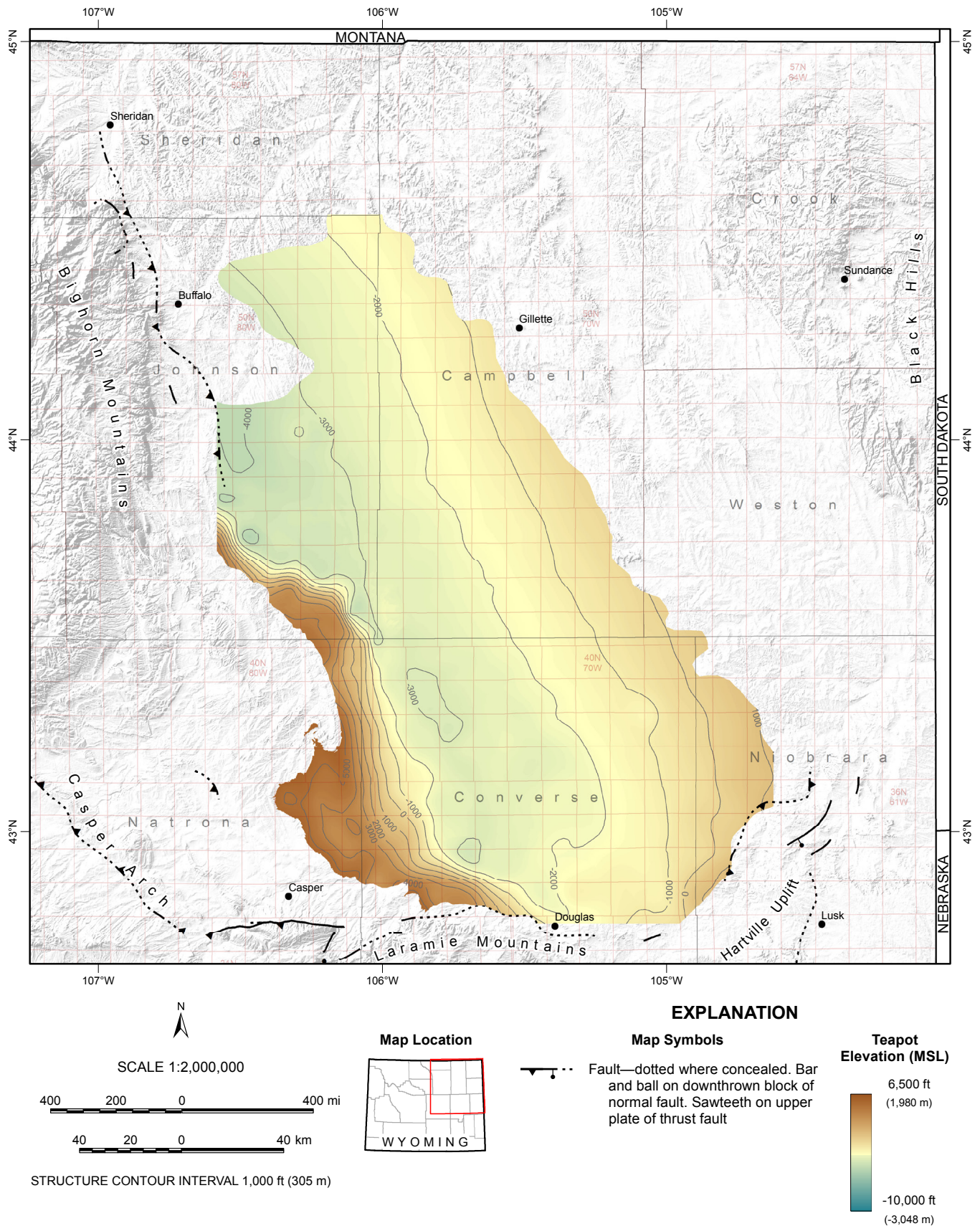


Figure 33. Structure map of top of the Teckla Sandstone Member of the Lewis Shale. Elevation is relative to mean sea level (MSL).

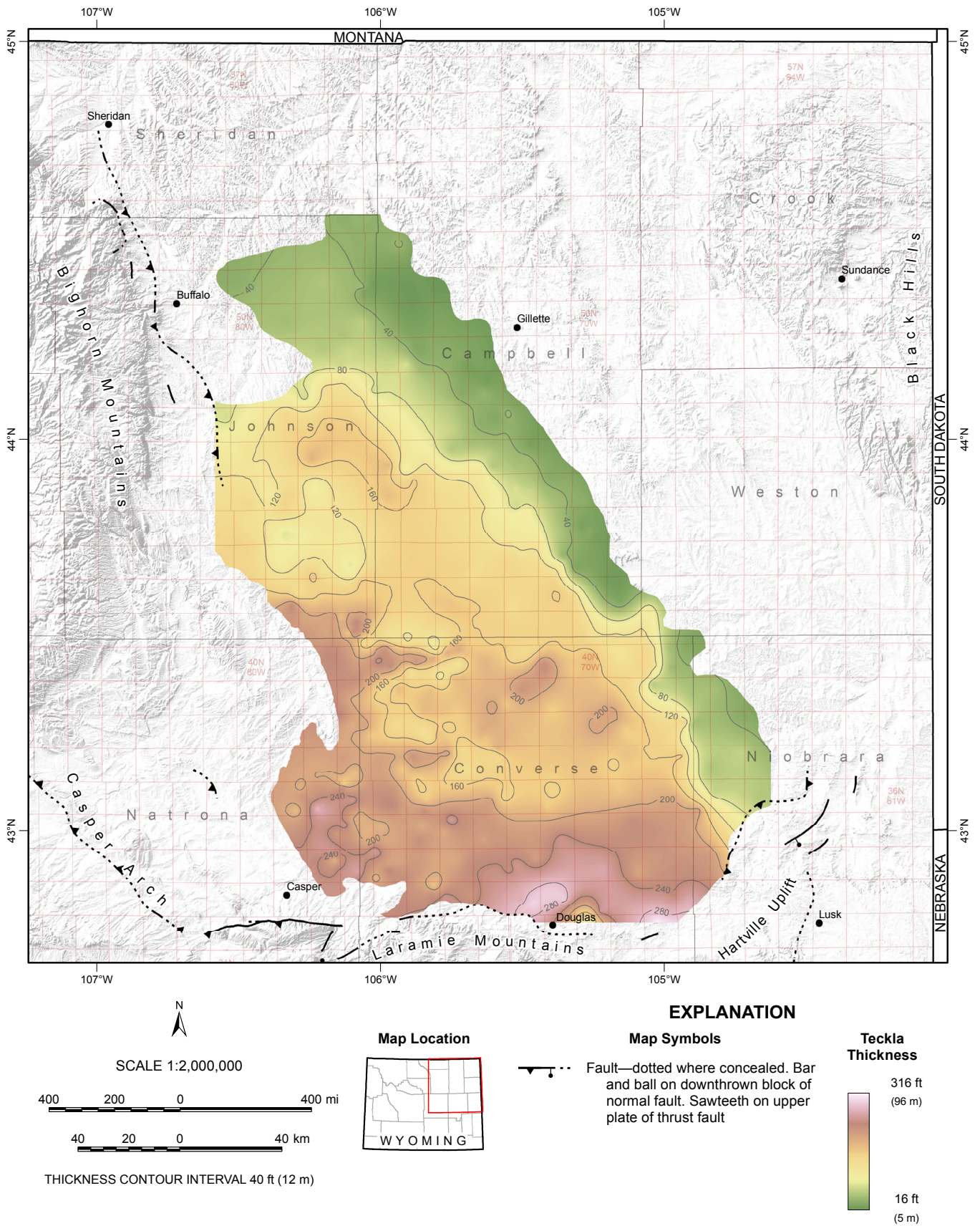


Figure 34. Thickness of the Teckla Sandstone Member of the Lewis Shale.

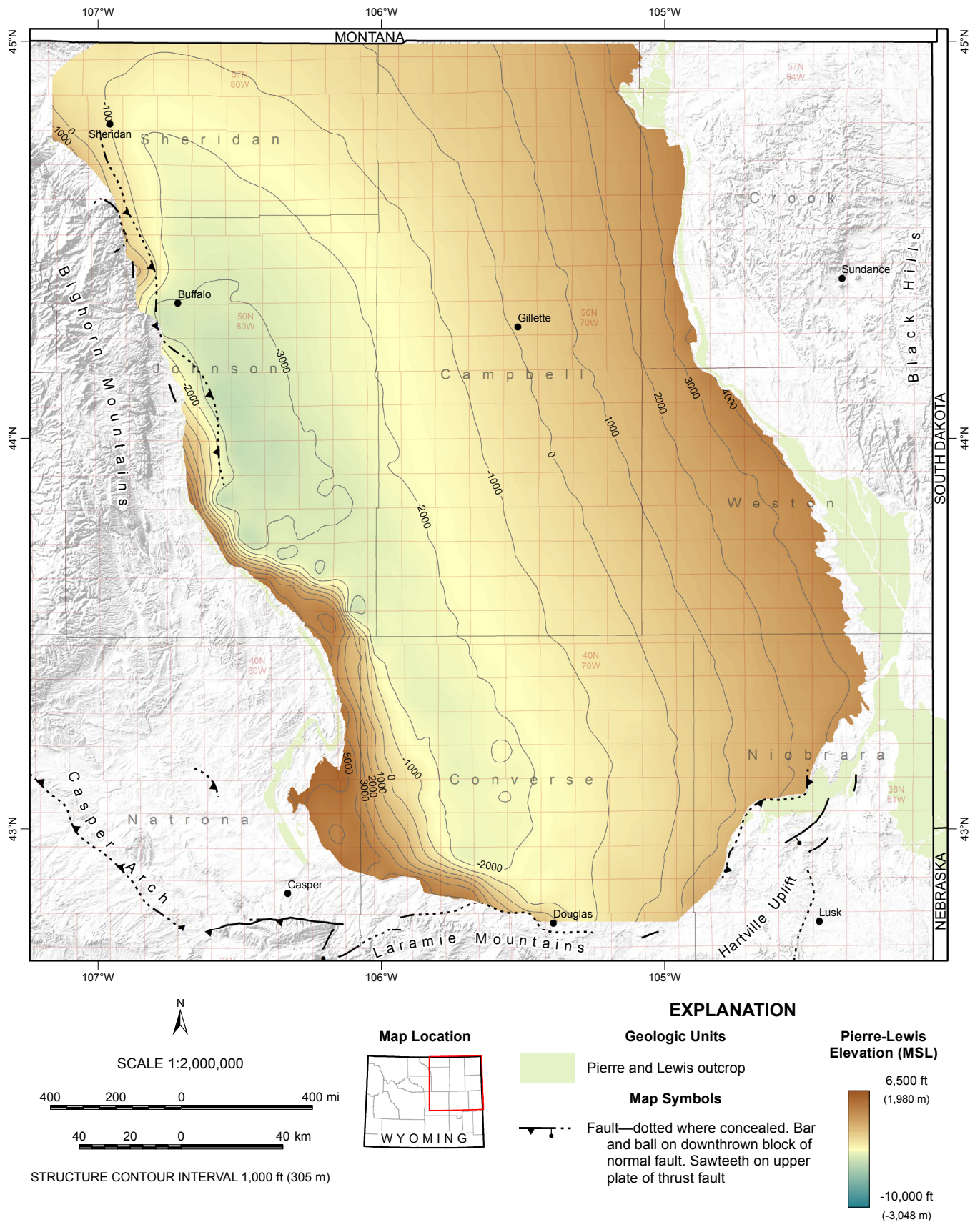


Figure 35. Structure map of base of the Fox Hills Sandstone (top of the combined Pierre Shale-Lewis Shale). Elevation is relative to mean sea level (MSL).

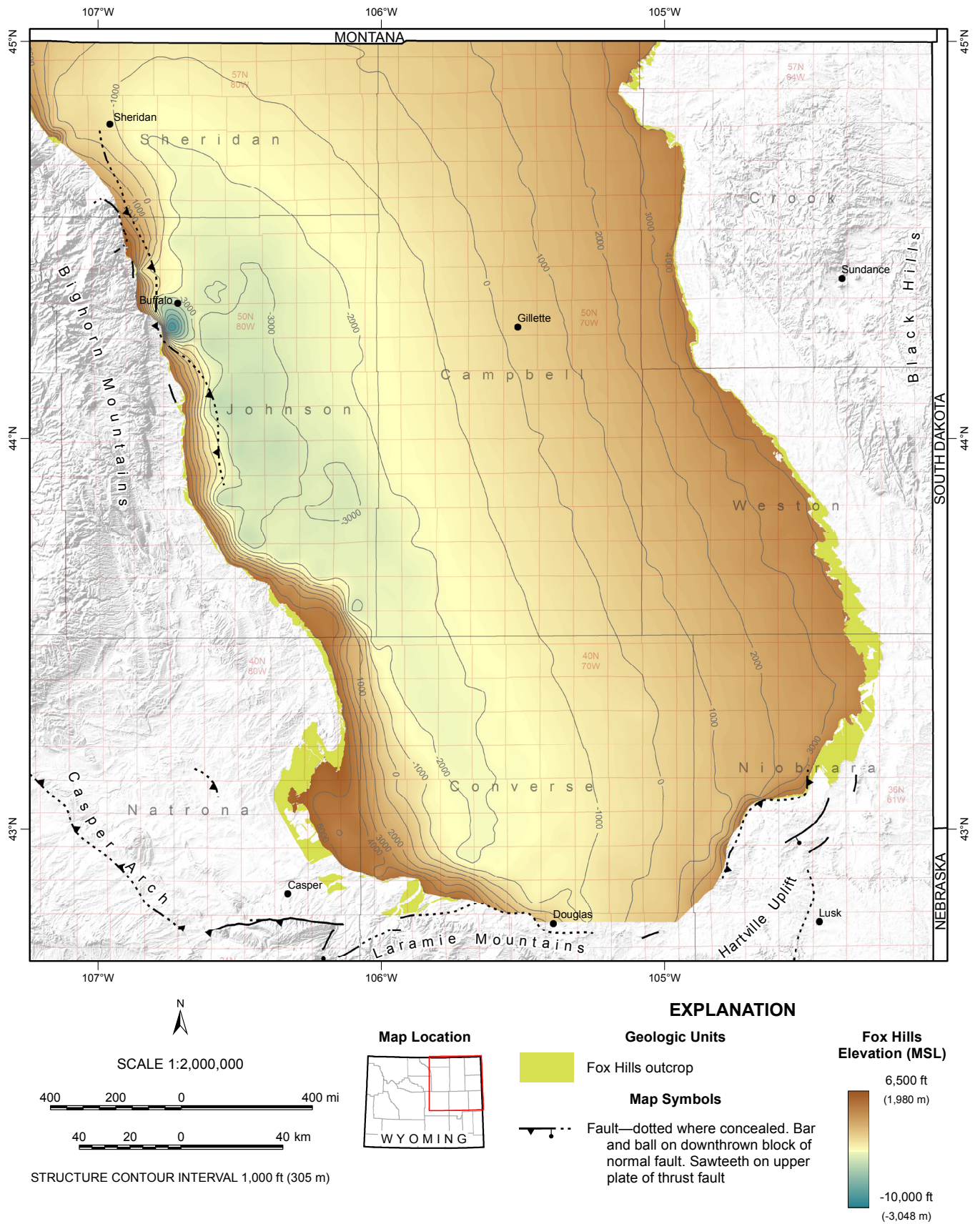


Figure 36. Structure map of top of the Fox Hills Sandstone. Elevation is relative to mean sea level (MSL).

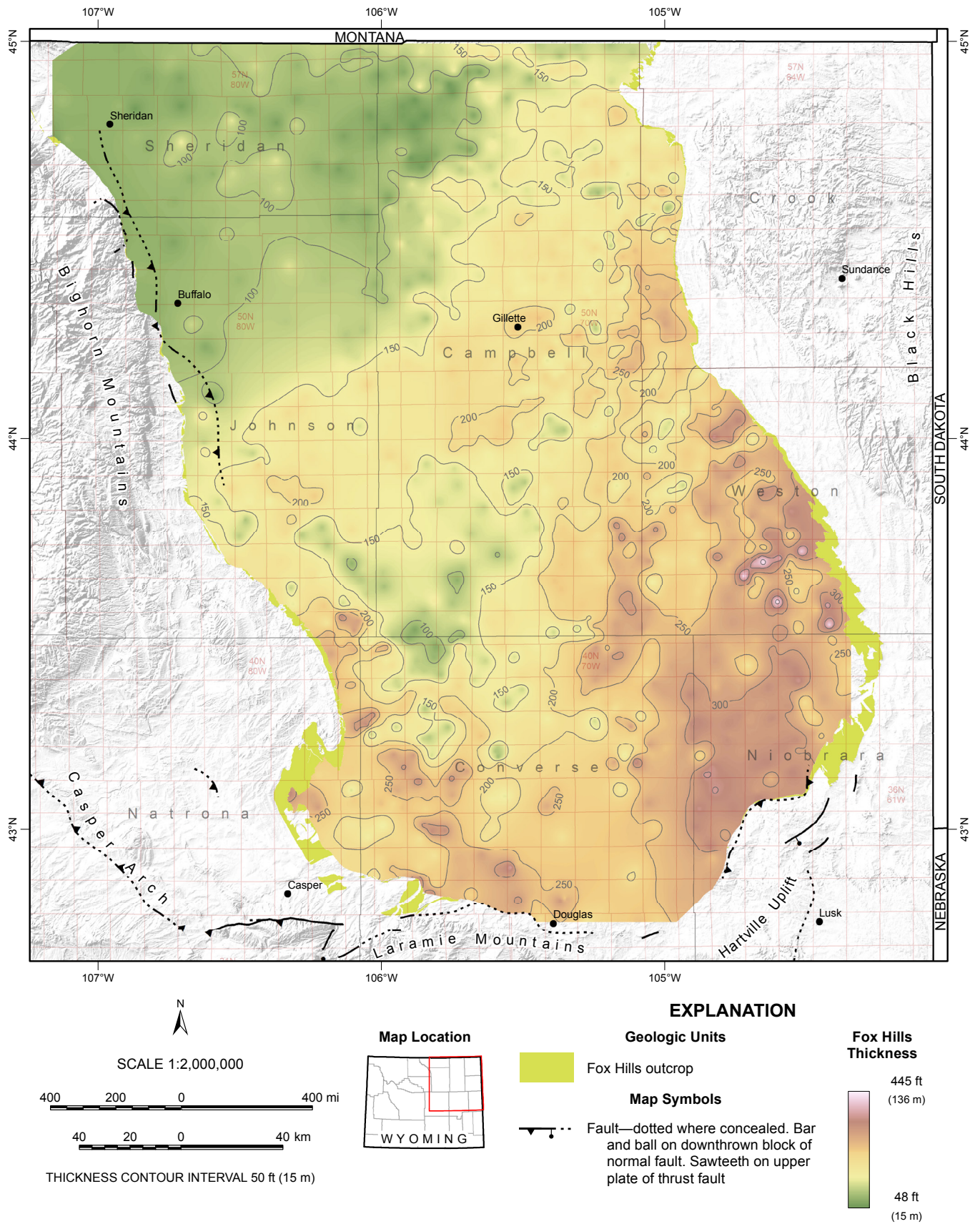


Figure 37. Thickness of the Fox Hills Sandstone.

SUMMARY

To better understand the PRB's prolific Upper Cretaceous hydrocarbon reservoirs, source rocks, and intervening strata, this study identified and correlated key stratigraphic horizons using geophysical logs from more than 2,200 oil and gas wells. Contour maps interpolated from the subsurface interpretations illustrate how the depth to and thickness of each formation varies spatially across the basin. Examination of spatial trends both within and between formations can provide insight into the depositional, structural, and hydrocarbon development history of this important oil- and gas-producing basin.

The database of well data, formation tops, and interpolated structure and thickness contours can be viewed online on the WSGS [Interactive Oil and Gas Map of Wyoming](#). Users can export formation tops and associated well data from the interactive map. The spatial well points and formation structure and thickness line and raster contours can be downloaded from a supplementary geodatabase on the WSGS [publications webpage](#).

The authors welcome input and discussion regarding the formation top interpretations, as we hope to continually refine and expand the dataset.

ACKNOWLEDGMENTS

This study was partially funded through the U.S. Geological Survey's National Coal Resources Data System (NCRDS) program on unconventional reservoirs (Grant G15AC00297). Assistance in picking well tops and database quality control was provided by Amy Freye, Jesse Pisel, and Martin Palkovic. Christina George edited the manuscript and provided layout. Thanks to all.

REFERENCES

- Anna, L.O., 2010, Geologic assessment of undiscovered oil and gas in the Powder River Basin province, Wyoming and Montana, *in* Total petroleum systems and geologic assessment of oil and gas resources in the Powder River Basin province, Wyoming and Montana: U.S. Geological Survey Digital Data Series DDS-69-U, chap. 1, 97 p. (Revised April 2010.)
- Berg, R.L., 1975, Depositional environment of Upper Cretaceous Sussex Sandstone, House Creek field, Wyoming: American Association of Petroleum Geologists Bulletin, v. 59, no. 11, p. 2,099-2,110.
- Blackstone, D.L., Jr., 1993, Precambrian basement map of Wyoming—Outcrop and structural configuration: Geological Survey of Wyoming [Wyoming State Geological Survey] Map Series 43, scale 1:1,000,000.
- Bottjer, R.J., Hendricks, M.L., Stright, D.H., and Bettridge, J.A., 2014, Sussex Sandstone, Hornbuckle trend, Powder River Basin, Wyoming—Lithofacies and reservoir properties in a tight oil play: AAPG Rocky Mountain Section Meeting, Denver, Colorado, July 20-22, 2014.
- Bottjer, R.J., Gustason, E.R., and Smith, K.H., 2017, Selected Rocky Mountain tight oil sandstone plays: Rocky Mountain Association of Geologists, Symposium and Core Workshop, October 26, 2017.
- Boyd, D.W., 1993, Paleozoic history of Wyoming, *in* Snoke, A.W., Steidtmann, J.R., and Roberts, S.M., eds., Geology of Wyoming: Geological Survey of Wyoming [Wyoming State Geological Survey] Memoir 5, p. 164-187.
- Brown, W.G., 1993, Structural style of Laramide basement-cored uplifts and associated folds, *in* Snoke, A.W., Steidtmann, J.R., and Roberts, S.M., eds., Geology of Wyoming: Geological Survey of Wyoming [Wyoming State Geological Survey] Memoir 5, p. 312-371.
- Cobban, W.A., 1951, Colorado shale of central and northwestern Montana and equivalent rocks of Black Hills: American Association of Petroleum Geologists Bulletin, v. 35, no. 10, p. 2,170-2,198.
- Cobban, W.A., 1952, Cretaceous rocks on the north flank of the Black Hills uplift, *in* Sonnenberg, P.P., ed., Black Hills-Williston Basin: Billings Geological Society Annual Field Conference, 3rd, September 4-7, 1952, Guidebook, p. 86-88.
- Cuddus, Yanet, Phillips, Dave, Will, Celina, Swager, Lee, Moore, W.R. Jr., Gbededo, Midowa, Del Castillo, Yanil, and Belobraydic, Matthew, 2019, Integrated assessment of the Niobrara and Mowry shale plays, Powder River Basin, Wyoming: AAPG Rocky Mountain Section Meeting, Cheyenne, Wyoming, September 15-18, 2019.
- Curry, W.H. III, 1976, Type section of the Teapot Sandstone, *in* Laudon, R.B., Curry, W.H. III, and Runge, J.S., eds., Geology and energy resources of the Powder River: Wyoming Geological Association, 28th annual field conference, Guidebook, p. 29-32.
- Dellenbach, J.T., 2019, Reservoir characterization and petroleum potential of the Upper Cretaceous Wall Creek Member of the Frontier Formation, western Powder River Basin, Wyoming: Golden, Colorado School of Mines, M.S. thesis, 109 p.
- Dolson, J.C., Muller, Dave, Evetts, M.J., and Stein, J.A., 1991, Regional paleotopographic trends and production, Muddy Sandstone (Lower Cretaceous), central and northern Rocky Mountains: American Association of Petroleum Geologists Bulletin, v. 75, p. 409-435.
- Dolton, G.L., Fox, J.E., and Clayton, J.L., 1990, Petroleum geology of the Powder River Basin, Wyoming and Montana: U.S. Geological Survey Open-File Report 88-450-P, 64 p.
- Eicher, D.L., 1962, Biostratigraphy of the Thermopolis, Muddy, and Shell Creek formations: Wyoming Geological Association, 17th annual field conference, Guidebook, p. 72-93.
- Fox, J.R., 1993a, Stratigraphic cross sections A-A' through F-F, showing electric logs of Upper Cretaceous and older rocks, Powder River Basin, Montana and Wyoming: U.S. Geological Survey Oil and Gas Investigations Chart OC-135.

- Fox, J.R., 1993b, Stratigraphic cross sections G-G' through L-L', showing electric logs of Upper Cretaceous and older rocks, Powder River Basin, Wyoming: U.S. Geological Survey Oil and Gas Investigations Chart OC-136.
- Fox, J.R., 1993c, Stratigraphic cross sections M-M' through R-R', showing electric logs of Upper Cretaceous and older rocks, Powder River Basin, Wyoming: U.S. Geological Survey Oil and Gas Investigations Chart OC-137.
- Fox, J.R., 1993d, Stratigraphic cross sections S-S' through V-V', showing electric logs of Upper Cretaceous and older rocks, Powder River Basin, Montana and Wyoming: U.S. Geological Survey Oil and Gas Investigations Chart OC-138.
- Gill, J.R., Cobban, W.A., and Kier, P.M., 1966, The Red Bird section of Upper Cretaceous Pierre Shale in Wyoming: U.S. Geological Survey Professional Paper 393-A, 69 p., 12 pls.
- Gill, J.R., and Cobban, W.A., 1973, Stratigraphy and geologic history of the Montana Group and equivalent rocks, Montana, Wyoming, and North and South Dakota: U.S. Geological Survey Professional Paper 776, 37 p.
- Hallberg, L.L., Lyman, R.M., Boyd, C.S., Jones, R.W., and Ver Ploeg, A.J., 2002, Geologic map of the Recluse 30' x 60' quadrangle, Campbell and Crook counties, Wyoming, and southeastern Montana: Wyoming State Geological Survey Map Series 60, scale 1:100,000.
- Hart, N.R., Dix, M.C., Mainali, P., Pukar, H.D., Morrell, Austin, and Matheny, Mei, 2019, Modeling mineralogy and total organic carbon (TOC) from X-ray fluorescence (XRF) elemental data for improved formation evaluation in the Powder River Basin: Unconventional Resources Technology Conference (URTeC), Denver, Colorado, July 22–24, 2019.
- Heger, A.W., 2016, Stratigraphy and reservoir characterization of the Turner Sandstone, southern Powder River Basin, Wyoming: Golden, Colorado School of Mines, M.S. thesis, 149 p.
- Hunter, John, Ver Ploeg, A.J., and Boyd, C.S., 2005, Geologic map of the Casper 30' x 60' quadrangle, Natrona and Converse counties, Wyoming: Wyoming State Geological Survey Map Series 65, scale 1:100,000.
- Johnson, J.F., and Micale, D.C., 2008, Geologic map of the Lance Creek 30' x 60' quadrangle, Niobrara and Converse counties, Wyoming, Fall River and Custer counties, South Dakota, and Sioux County, Nebraska: Wyoming State Geological Survey Map Series 79, scale 1:100,000.
- Kaykun, Armagan, 2018, Sequence stratigraphy of the lower Pierre Shale of the southern Powder River Basin—A ramp margin sequence that terminates Niobrara Formation carbonate deposition: Interpretation, v. 6, no. 1, SA7–SA13.
- Kegel, Jason, Miranda, Ted, Lenz, Nathan, Keay, James, and O'Reilly, Cian, 2019, Powder River Basin production review from 2011 through 2018—How refinements in completions and operations have led to increasing production in the Upper Cretaceous formations of Campbell and Converse counties, Wyoming: Unconventional Resources Technology Conference (URTeC), Denver, Colorado, July 22–24, 2019.
- Kondakci, E.C., 2019, Geologic reservoir characterization of the Niobrara Formation in the Trabling field, western Powder River Basin, Wyoming: Golden, Colorado School of Mines, M.S. thesis, 215 p.
- Landon, S.M., Longman, M.W., and Luneau, B.A., 2001, Hydrocarbon source rock potential of the Upper Cretaceous Niobrara Formation, Western Interior Seaway of the Rocky Mountain Region: The Mountain Geologist, v. 38, no. 1, p. 1–18.
- Lillegraven, J.A., 1993, Correlation of Paleogene strata across Wyoming—A user's guide, *in* Snoke, A.W., Steidtmann, J.R., and Roberts, S.M., eds., Geology of Wyoming: Geological Survey of Wyoming [Wyoming State Geological Survey] Memoir 5, p. 415–477.
- Love, J.D., and Christiansen, A.C., comps., 1985, Geologic map of Wyoming: U.S. Geological Survey, 3 sheets, scale 1:500,000. (Re-released 2014, Wyoming State Geological Survey.)
- Lynds, R.M., and Slattery, J.S., 2017, Correlation of the Upper Cretaceous strata of Wyoming: Wyoming State Geological Survey Open File Report 2017-3.

- Macdonald, R.H., and Byers, C.W., 1988, Depositional history of the Greenhorn Formation (Upper Cretaceous), northwestern Black Hills: *The Mountain Geologist*, v. 25, no. 3, p. 71–85.
- McLaughlin, J.F., Stafford, J.E., and Harris, R.E., 2011, Geologic map of the Lusk 30' x 60' quadrangle, Niobrara, Goshen, Converse, and Platte counties, Wyoming, and Sioux County, Nebraska: Wyoming State Geological Survey Map Series 82, scale 1:100,000.
- McLaughlin, J.F., and Ver Ploeg, A.J., 2006, Geologic map of the Newcastle 30' x 60' quadrangle, Weston and Niobrara counties, Wyoming, and Pennington and Custer counties, South Dakota: Wyoming State Geological Survey Map Series 71, scale 1:100,000.
- McLaughlin, J.F., and Ver Ploeg, A.J., 2008, Geologic map of the Douglas 30' x 60' quadrangle, Converse and Platte counties, Wyoming: Wyoming State Geological Survey Map Series 83, scale 1:100,000.
- Merewether, E.A., 1980, Stratigraphy of mid-Cretaceous formations at drilling sites in Weston and Johnson counties, northeastern Wyoming: U.S. Geological Survey Professional Paper 1186-A, 25 p.
- Merewether, E.A., 1996, Stratigraphy and tectonic implications of Upper Cretaceous rocks in the Powder River Basin, northeastern Wyoming and southeastern Montana: U.S. Geological Survey Bulletin 1917-T, 92 p.
- Merewether, E.A., Cobban, W.A., Matson, R.M., and Magathan, W.J., 1977a, Stratigraphic diagrams with electric logs of Upper Cretaceous rocks, Powder River Basin, Natrona, Campbell, and Weston counties, Wyoming, section B-B': U.S. Geological Survey Oil and Gas Investigations Map OC-74.
- Merewether, E.A., Cobban, W.A., Matson, R.M., and Magathan, W.J., 1977b, Stratigraphic diagrams with electric logs of Upper Cretaceous rocks, Powder River Basin, Natrona, Converse, and Niobrara Counties, Wyoming, section C-C': U.S. Geological Survey Oil and Gas Investigations Map OC-75.
- Merewether, E.A., Cobban, W.A., Matson, R.M., and Magathan, W.J., 1977c, Stratigraphic diagrams with electric logs of Upper Cretaceous rocks, Powder River Basin, Sheridan, Johnson, Campbell, and Converse Counties, Wyoming, section D-D': U.S. Geological Survey Oil and Gas Investigations Map OC-76.
- Merewether, E.A., Cobban, W.A., and Obradovich, J.D., 2007, Regional unconformities in Turonian and Coniacian (Upper Cretaceous) strata in Colorado, Wyoming, and adjoining states—Biochronological evidence: *Rocky Mountain Geology*, v. 42, no. 2, p. 95–122.
- Merewether, E.A., Cobban, W.A., and Cavanaugh, E.T., 1979, Frontier Formation and equivalent rocks in eastern Wyoming: *The Mountain Geologist*, v. 6, no. 3, p. 67–102.
- Momper, J.A., and Williams, J.A., 1984, Geochemical exploration in the Powder River Basin, *in* Demaison, Gerard, and Murriss, R.J., eds., *Petroleum geochemistry and basin evaluation*: American Association of Petroleum Geologists Memoir 35, p. 181–191.
- Olea, R.A., 2009, A practical primer on geostatistics: U.S. Geological Survey Open-File Report 2009-1103, ver. 1.0, 346 p. (Revised December 2018, ver. 1.4)
- Oliver, M.A., and Webster, Richard, 2014, A tutorial guide to geostatistics—Computing and modelling variograms and kriging: *CATENA*, v. 113, p. 56–69.
- Picard, M.D., 1993, The early Mesozoic history of Wyoming, *in* Snoke, A.W., Steidtmann, J.R., and Roberts, S.M., eds., *Geology of Wyoming*: Geological Survey of Wyoming [Wyoming State Geological Survey] Memoir 5, p. 210–248.
- Purvis, S.V., Iwobi, Christopher, Kenny, R.M., Fenton, J.P.G., Pandey, Vishnu, and Davies, C.J., 2017, Facies control on the prospectivity of the unconventional Mowry Formation, southern Powder River Basin, Wyoming, USA: Unconventional Resources Technology Conference, Austin, Texas, July 24–26, 2017.
- Rahman, M.W., Olson, R.K., Symcox, C.W., and Bingman, Sean, 2016, Geochemistry of Cretaceous oils and source rocks in the Powder River Basin: Unconventional Resources Technology Conference (URTeC), San Antonio, Texas, August 1–3, 2016.

- Robinson, C.S., Mapel, W.J., and Bergendahl, M.H., 1964, Stratigraphy and structure of the northern and western flanks of the Black Hills Uplift, Wyoming, Montana, and South Dakota: U.S. Geological Survey Professional Paper 404, 134 p.
- Royse, Frank, Jr., 1993, An overview of the geologic structure of the thrust belt in Wyoming, northern Utah, and eastern Idaho, *in* Snoke, A.W., Steidtmann, J.R., and Roberts, S.M., eds., *Geology of Wyoming: Geological Survey of Wyoming* [Wyoming State Geological Survey] Memoir 5, p. 272–311.
- Runge, J.S., Wicker, W.L., and Eckelberg, D.J., 1973, A subsurface type section of the Teckla Sand Member of the Lewis Shale Formation: *Wyoming Geological Association Earth Science Bulletin*, v. 6, no. 3, p. 3–18.
- Sonnenberg, S.A., 2018, The Niobrara Formation in the southern Powder River Basin, Wyoming—An emerging giant continuous petroleum accumulation: *First Break*, v. 36, no. 3, p. 37–45.
- Steidtmann, J.R., 1993, The Cretaceous foreland basin and its sedimentary record, *in* Snoke, A.W., Steidtmann, J.R., and Roberts, S.M., eds., *Geology of Wyoming: Geological Survey of Wyoming* [Wyoming State Geological Survey] Memoir 5, p. 250–271.
- Steidtmann, Matthew, 2019, Incised valleys in the Parkman sandstone at Teapot Dome, Wyoming—A comprehensive outcrop analysis: Golden, Colorado School of Mines, M.S. thesis, 104 p.
- Stewart, Torell, 2019, Reservoir characterization of the B and C Niobrara benches in the southern Powder River Basin, in Converse and Campbell counties, Wyoming: Golden, Colorado School of Mines, M.S. thesis, 165 p.
- Sutherland, W.M., 2007, Geologic map of the Sundance 30' x 60' quadrangle, Crook and Weston counties, Wyoming, and Lawrence and Pennington counties, South Dakota: Wyoming State Geological Survey Map Series 78, scale 1:100,000.
- Sutherland, W.M., 2008, Geologic map of the Devils Tower 30' x 60' quadrangle, Crook County, Wyoming, Butte and Lawrence counties, South Dakota, and Carter County, Montana: Wyoming State Geological Survey Map Series 81, scale 1:100,000.
- Taylor, James, 2012, Petroleum system analysis of the Niobrara Formation in the southern Powder River Basin: Golden, Colorado School of Mines, M.S. thesis, 164 p.
- Taylor, James, and Sonnenberg, S.A., 2014, Reservoir characterization of the Niobrara Formation, southern Powder River Basin, Wyoming: *The Mountain Geologist*, v. 51, no. 1, p. 83–108.
- Tillman, R.W., and Martinsen, R.S., 1984, The Shannon shelf-ridge sandstone complex, Salt Creek anticline area, Powder River Basin, Wyoming, *in* Tillman, R.W., and Siemers, C.T., eds., *Siliciclastic shelf sediments: Society of Economic Paleontologists and Mineralogists Special Publication 34*, p. 85–142.
- Toner, R.N., 2019, Influences on oil and natural gas production from the Wall Creek and Turner sandstone reservoirs, Powder River Basin, Wyoming: Wyoming State Geological Survey Report of Investigations 77, 84 p., online map at wsgs.maps.arcgis.com/apps/webappviewer/index.html?id=d00fe805fdf04db3b25eb3b56d81a953.
- Toner, R.N., Lynds, R.M., and Stafford, J.E., 2019, Oil and gas map of Wyoming: Wyoming State Geological Survey Map Series 104, scale 1:500,000.
- U.S. Geological Survey, 2009, Digital elevation model for Wyoming at 10 meters: U.S Geological Survey National Elevation Data, accessed April 2020, at <https://viewer.nationalmap.gov/basic/>.
- Van Wagoner, J.C., Mitchum, R.M., Campion, K.M., and Rahmanian, V.D., 1990, Siliciclastic sequence stratigraphy in well logs, cores, and outcrops Concepts for high-resolution correlation of time and facies: *American Association of Petroleum Geologists Methods in Exploration Series*, no. 7, 55 p.
- Ver Ploeg, A.J., and Boyd, C.S., 2002, Geologic map of the Buffalo 30' x 60' quadrangle, Johnson and Campbell counties, Wyoming: Wyoming State Geological Survey Map Series 59, scale 1:100,000.

- Ver Ploeg, A.J., and Boyd, C.S., 2003, Geologic map of the Sheridan 30' x 60' quadrangle, Sheridan, Johnson, and Campbell counties, Wyoming, and southeastern Montana: Wyoming State Geological Survey Map Series 64, scale 1:100,000.
- Ver Ploeg, A.J., Boyd, C.S., and Mulbay, J.M., 2004, Geologic map of the Kaycee 30' x 60' quadrangle, Johnson, and Campbell counties, Wyoming: Wyoming State Geological Survey Map Series 63, scale 1:100,000.
- Weimer, R.J., and Flexer, Akiva, 1985, Depositional patterns and unconformities, Upper Cretaceous, eastern Powder River Basin, Wyoming, *in* Nelson, G.E., ed., The Cretaceous geology of Wyoming: Wyoming Geological Association, 36th annual field conference, Guidebook, p. 131–147.
- Wittke, S.J., 2007, Geologic map of the Midwest 30' x 60' quadrangle, Natrona, Converse, Johnson, and Campbell counties, Wyoming: Wyoming State Geological Survey Map Series 73, scale 1:100,000.
- Wyoming Oil and Gas Conservation Commission, 2020, Well header and production data download, accessed April 2020, at <http://pipeline.wyo.gov/legacywogcce.cfm>.
- Zborowski, Matt, 2018, It may be boom time for the oil-rich Powder River Basin: *Journal of Petroleum Technology* v. 70, no. 10, 5 p.

